THESIS FOR THE DEGREE OF DOCTOR OF PHILOSOPHY IN SOLID AND STRUCTURAL MECHANICS

Scattering of elastic waves by an anisotropic sphere with application to polycrystalline materials

ATA JAFARZADEH

Department of Mechanics and Maritime Sciences

Dynamics

CHALMERS UNIVERSITY OF TECHNOLOGY

Göteborg, Sweden 2023

Scattering of elastic waves by an anisotropic sphere with application to polycrystalline materials

ATA JAFARZADEH
ISBN 978-91-7905-914-9

Doktorsavhandlingar vid Chalmers tekniska högskola
Ny serie nr. 5380
ISSN 0346-718X
Department of Mechanics and Maritime Sciences
Dynamics
Chalmers University of Technology
SE-412 96 Göteborg
Sweden
Telephone: +46 (0)31-772 1000

Cover:
Wave scattering by a spherical obstacle.
Illustrator: Asieh Baghishani

Chalmers Reproservice
Göteborg, Sweden 2023

Scattering of elastic waves by an anisotropic sphere with application to polycrystalline materials

ATA JAFARZADEH
Department of Mechanics and Maritime Sciences
Dynamics
Chalmers University of Technology

Abstract

Scattering of a plane wave by a single spherical obstacle is the archetype of many scattering problems in various branches of physics. Spherical objects can provide a good approximation for many real objects, and the analytic formulation for a single sphere can be used to investigate wave propagation in more complex structures like particulate composites or grainy materials, which may have applications in non-destructive testing, material characterization, medical ultrasound, etc. The main objective of this thesis is to investigate an analytical solution for scattering of elastic waves by an anisotropic sphere with various types of anisotropy. Throughout the thesis a systematic series expansion approach is used to express displacement and traction fields outside and inside the sphere. For the surrounding isotropic medium such an expansion is made in terms of the traditional vector spherical wave functions. However, describing the fields inside the anisotropic sphere is more complicated since the classical methods are not applicable. The first step is to describe the anisotropy in spherical coordinates, then the expansion inside the sphere is made in the vector spherical harmonics in the angular directions and power series in the radial direction. The governing equations inside the sphere provide recurrence relations among the unknown expansion coefficients. The remaining expansion coefficients outside and inside the sphere can be found using the boundary conditions on the sphere. Thus, this gives the scattered wave coefficients from which the transition (**T**) matrix can be found. This is convenient as the **T** matrix fully describes the scattering by the sphere and is independent of the incident wave. The expressions of the general **T** matrix elements are complicated, but in the low frequency limit it is possible to obtain explicit expressions.

The **T** matrices may be used to solve more complex problems like the wave propagation in polycrystalline materials. The attenuation and wave velocity in a polycrystalline material with randomly oriented anisotropic grains are thus investigated. These quantities are calculated analytically using the simple theory of Foldy and show a very good correspondence for low frequencies with previously published results and numerical computations with FEM. This approach is then utilized for an inhomogeneous medium with local anisotropy, incorporating various statistical information regarding the geometrical and elastic properties of the inhomogeneities.

Keywords: Scattering, Spherical obstacle, Anisotropy, **T** matrix, Polycrystalline materials, Effective wave number, Attenuation, Phase velocity.

To my wife, Asieh.

Preface

The central focus of this thesis is to look into the intricate interaction of elastic waves with anisotropic spherical objects, thereby advancing our understanding of wave scattering phenomena. The research is conducted at the Division of Dynamics within the Department of Mechanics and Maritime Sciences at Chalmers University of Technology between December 2018 and August 2023. This research was funded by the Swedish Research Council, and I gratefully acknowledge their support.

Acknowledgements

I stand here at the end of a journey, one that was covered with challenges, friendships, and unforgettable memories. Let me start by thanking my supervisors, Peter Folkow and Anders Boström. They were not just my supervisors; they were guides and mentors in the best way. Their unwavering support, trust, and patience through thick and thin gave me the freedom to find my own balance and direction through my career and life.

I would also like to mention the friendships I have had, as this journey was not only focused around equations and papers. I extend my gratitude to my colleagues at the Dynamics and Material and Computational Mechanics divisions. From office pranks that turned mundane days into hilarious adventures to the countless moments we shared during fika breaks, your presence has meant much more than just professional connections. Our adventures outside the university and all the gatherings often with remembering incidents added a layer of joy to this academic journey that I will forever cherish. I very much like to stay connected and share more awesome times with all of you.

Of course the past five years was not just professional it was also deeply personal. I would like to thank my incredible wife, Asieh, whose support exceed imagination. Your constant encouragement, love, and understanding sustained me through the late nights, the tough days, and the moments of doubt. Your patience during the storm of research is something I can never repay.

In closing, I am very thankful to my parents Jalal and Safa, brother, and my family in-law. Their belief in me never wavered. Their pride in my every little achievement filled my days with strength and resolve.

Thesis

This thesis consists of an extended summary and the following appended papers:

Paper A A. Jafarzadeh, P. D. Folkow, and A. Boström. "Scattering of elastic SH waves by transversely isotropic sphere". *Proceedings of the International Conference on Structural Dynamic , EURODYN*. vol. 2. 2020, pp. 2782–2797

Paper B A. Jafarzadeh, P. D. Folkow, and A. Boström. Scattering of elastic waves by a transversely isotropic sphere and ultrasonic attenuation in hexagonal polycrystalline materials. *Wave Motion* **112** (2022), 102963

Paper C A. Jafarzadeh, P. D. Folkow, and A. Boström. Scattering of elastic waves by a sphere with cubic anisotropy with application to attenuation in polycrystalline materials. *Proceedings of the Royal Society A: Mathematical, Physical and Engineering Sciences* **479**.2272 (2023), 20220476

Paper D A. Jafarzadeh, P. D. Folkow, and A. Boström. Scattering of elastic waves by a sphere with orthorhombic anisotropy and application to polycrystalline material characterization. *Submitted for international publication* (2023)

Paper E A. Jafarzadeh, P. D. Folkow, and A. Boström. Low frequency wave propagation in multiphase polycrystalline materials. *To be submitted for international publication* (2023)

Contributions to co-authored papers

The appended papers were prepared in collaboration with the co-authors. The author of this thesis was responsible for the major progress of the work, including the following tasks

- **Papers A-D:** Taking part in planning the paper and developing the theory, performing analytical derivations and numerical evaluations, writing the paper, managing the submission and peer-review process.
- **Paper E:** Providing the fundamental concepts, shaping the direction of the paper, developing the theory, performing analytical derivations and numerical evaluations, writing the paper.

Contents

Part I

Extended Summary

1 Introduction

Wave propagation in elastic solids with inhomogeneities is an interesting and extensive research field. The findings in this subject have numerous applications in diverse engineering fields, including material characterization, nondestructive materials testing using ultrasound, in-situ safety and reliability control of complex structural components through acoustic emission, dynamic fracture mechanics, seismology, and ground vibrations. Among these subjects, the current study primarily focuses on specific areas closely related to material characterization and nondestructive testing.

1.1 Background and motivation

Engineering materials often contain various types of inhomogeneities, hereafter referred to as obstacles. These obstacles can appear as micro grains within metals, as well as cracks, cavities in materials, and fibers and particles within composite materials. Such obstacles can arise either naturally or as a result of materials processing, manufacturing, and in-service conditions. Detecting and characterizing these obstacles is crucial in engineering applications as they significantly impact the integrity, stiffness, and strength of the material. Nondestructive testing techniques are commonly employed for this purpose. These techniques often involve emitting some type of waves into a medium and studying their propagation. This approach is highly valuable for material characterization, because there is a direct correlation between material properties, such as distribution, density, location, size, and orientation of the obstacles with the characteristics of the wave when propagating through the medium, such as effective wave speed and intensity.

In contrast to wave propagation in ideally homogeneous elastic solids, waves propagating in elastic solids with obstacles generally experience diffraction and scattering. Diffraction refers to the deviation of the wave from its original path, while scattering refers to the wave radiation from the obstacle. The diffraction and scattering of the incident wave give rise to interesting phenomena in the medium. When an incident wave propagates inside a medium, it carries energy. However, in the presence of obstacles, this energy is converted into scattered wave energy. As a result, the incident wave experiences intensity reduction and shape distortion, leading to attenuation and dispersion. Therefore, even though the medium and obstacles are perfectly elastic and do not dissipate energy, an elastic solid with elastic obstacles appears as an attenuative and dispersive medium to an incident wave [1]. It is important to note that wave attenuation and dispersion can be influenced by factors other than scattering, but in this context, only the scattering effect is considered.

The analysis of scattering by a single obstacle has long served as a fundamental prerequisite for studying a medium containing a multitude of obstacles in various analytical methodologies. Scattering of waves by a single obstacle is a fundamental problem in various branches of mathematical physics, including acoustics, electromagnetics, and elasticity. Despite the differences between these fields, the basic nature of the problem remains the same: a propagating wave encounters a discontinuity in the form of an obstacle. Techniques employed to investigate such problems in elasticity typically draw from successful approaches used in acoustics and electromagnetics, such as separation-of-variables, **T** matrix methods, integral equation methods, and finite element methods (FEM). However, elastodynamic fields exhibit distinctive characteristics, including coupled wave equations and the presence of two wave speeds. Such properties increase the complexity of the elastodynamic equations. Therefore, most of the studies in elastic fields are limited to isotropic materials, which results in relative ease in mathematical treatment and still has important applications since many materials are approximately isotropic or can be homogenized as an isotropic material. A comprehensive overview of scattering of acoustic, electromagnetic, and elastic waves in isotropic media is covered in the literature [2, 3]. However, recent investigations of anisotropic materials, like composites, biological materials and grainy materials (typically metals), have demonstrated the importance of studying wave propagation in a medium with anisotropy.

Wave propagation in a medium with anisotropic obstacles is more complicated to study since many of the classical methods are not applicable any longer. Scattering by anisotropic obstacles has mostly been studied for electromagnetic waves [4, 5, 6]. For mechanical waves, most of the studies are performed for spherically and cylindrically anisotropic obstacles [7, 8, 9, 10, 11]. Scattering of elastic waves by an anisotropic obstacle when the anisotropy is in Cartesian coordinates is investigated in 2D by Boström [12, 13]. The method presented there is pursued in the present thesis to extend the possible solutions to 3D problems.

The analysis of multiple scattering has also been extensively pursued. Theoretically, a sequence of equations moving from single obstacle scattering to the inclusion of two-obstacle interactions, then three-obstacle interactions and upwards can be set up using, for instance, the **T** matrix method. However, the complexity of the equations increases in each step and thus it is normally pursued only for two obstacles [14] and is mostly limited to isotropic obstacles. On the other hand, there is a wide range of materials that contain or consist of a random distribution of anisotropic obstacles. Investigating the detailed structure of such materials involves dealing with a large number of parameters and leads to highly complex equations. However, in practical applications, such a detailed investigation is often unnecessary. Instead, it is more efficient to describe these materials using statistical characteristics, such as the density and size distribution of the obstacles.

Traditionally, the analysis of scattering in these structures has involved approximating the discrete medium with a continuous random inhomogeneous medium. The formal approach for studying such a medium usually involves employing volume integral equation methods in combination with perturbation methods. Although anisotropy of the medium greatly complicates the mathematical formalism, the fundamental concepts for analyzing wave propagation in these media remain the same as in simpler isotropic cases [15]. This method has been commonly employed to investigate the scattering problem and determine the attenuation and wave speed in granular materials, including simple or complex polycrystals with different types of grain anisotropy [15, 16, 17, 18]. However, these studies all seem to have restrictions to more or less weak anisotropy. In chapter 4, a more detailed exploration of this approach is provided.

Another approach for estimating the effective homogenized properties of random inhomogeneous materials is to utilize the scattering characteristics exhibited by individual obstacles. The scattering characteristic is typically tied to the energy carried by the wave as it scatters off each obstacle. Therefore, these obstacles can be considered secondary radiation sources referred to as scatterers, being stimulated by the incident waves. In some approximate methods, such as the theory of Foldy [19], the scattering characteristic of the individual scatterers, along with their statistical information, is utilized to calculate the effective wave number of the homogenized medium. This approach has been employed to estimate the attenuation of 2D polycrystalline materials with orthotropic grain properties [20] and is followed in this study for 3D cases. These approximate methods have demonstrated fewer limitations regarding the degree of anisotropy. However, they are usually constrained to specific statistical information concerning the size and distribution of obstacles. For example, they are applicable to a dilute distribution of obstacles or small-sized obstacles relative to the wavelength of the propagating wave (also known as low frequencies).

In addition to these analytical approaches, numerical methods like the Finite Element Method (FEM) have been recently employed to study polycrystalline materials and investigate their attenuation and phase velocity. Numerical approaches offer the advantage of capturing more complex and realistic scenarios, allowing for the inclusion of multiple scattering and addressing a wider range of anisotropy [21, 22, 23, 24, 25, 26, 27, 28]. These studies provide valuable information for exploring the behavior of polycrystalline materials in more detail. However, it is important to note that FEM cannot provide analytical expressions or closed form solutions, which often give valuable insights into the studied phenomena. Additionally, FEM is subject to limitations in terms of time and computational costs, also uncertainties regarding spatial discretization, boundary and loading conditions which can restrict its practicality and efficiency.

The main aim of the present thesis is to extend the possible type of analytical solutions by solving the canonical 3D problem of scattering of elastic waves by an anisotropic obstacle. The obstacle has a spherical shape and its material properties are assumed to be transversely isotropic, cubic or orthotropic. Meanwhile, the surrounding material is considered to be isotropic. A general solution may be presented by calculating the linear relationship between the expansion coefficient of the incident wave with those of the scattered wave in the spherical basis. Such a relation defines the transition $\mathbf{T}$ matrix of the sphere. This is pursued in the appended papers, first for a transversely isotropic sphere in Papers A and B. In Paper A, the problems is considered for a situation when there is only a torsional wave incident along the symmetry axis of the anisotropic sphere. Therefore the problem is simplified to an axisymmetric scalar situation. Using the same methodology in Paper B, the scattering of elastic waves by a transversely isotropic sphere with an arbitrary incident wave is studied. This is extended to the scattering by a sphere with cubic and orthotropic anisotropy in Paper C and D, respectively. In these papers the **T** matrix is calculated and presented explicitly for low frequencies. The **T** matrix can then be used to calculate the scattering for any incident wave, a plane wave, a wave from an ultrasonic probe, etc. The **T** matrix can also be used as a tool when considering multiple scattering problems, like the scattering by two or more spheres, or the scattering by a sphere close to a planar interface.

Another important purpose of the project is to use the **T** matrix to study grainy structured materials in which the grains can serve as scatterers. Specifically, the **T** matrix may be used to calculate the attenuation and effective wave speed in these materials as long as the correlation among scatterers may be neglected. Such an assumption may be reasonable for the cases with low concentrations of the grains or very small scattering by each grain. This purpose is pursued in Papers B-D for single phased equiaxed polycrystalline materials with various anisotropy symmetry of grains. Similarly, Paper E explores wave propagation in single phase and multiphase polycrystalline materials with a distribution of grain size.

1.2 Outline of the thesis

The extended summary of this thesis is structured as follows.

In chapter 2, the elastodynamic relations describing a scattering problem are introduced for general anisotropic materials. Then some special cases including isotropic, orthotropic, cubic and transversely isotropic materials are introduced and their effect on the elastodynamic wave equations is discussed. Furthermore, the transformation of the wave equations into a spherical coordinate system is explained. The study of spherical waves is then presented, focusing on the derivation of the general solution of the wave equations for isotropic materials. The solutions are expressed in terms of vector wave functions, providing a comprehensive representation of the wave behavior in isotropic materials in spherical coordinates.

Chapter 3 focuses on different scattering problems, specifically when the obstacle is not isotropic. An analytical approach to derive the solution in terms of the **T** matrix is discussed. First the general approach to study scattering of an arbitrary plane wave by an anisotropic sphere is outlined. Then the scalar case of a torsional wave scattering by a transversely isotropic sphere is explained giving more details.

Chapter 4 provides a brief exposition of approximate methods for studying wave propagation in materials with a random distribution of scatterers. It then focuses on their application to analyse grainy structures, particularly polycrystalline materials. This leads to estimates of effective properties like wave attenuation and phase velocity, offering insight into the behavior of such materials.

A summary of the appended papers is presented in chapter 5, followed by some concluding remarks and ideas for future work in chapter 6.

2 Elastodynamics

In this section, an outline is given of the principles of elasticity that are relevant to elastic wave propagation and scattering. This includes stress and strain definitions, constitutive relations, and governing equations. Isotropic media are in particular treated and some anisotropic media are also introduced. The elastodynamic problem is expressed in spherical coordinates and the corresponding vector wave functions are introduced. There is a wide body of literature that covers several aspects of continuum mechanics and elastic wave propagation ([29, 30]). One can refer to them for comprehensive explanations of the concepts discussed in this section.

2.1 Basic equations

To start developing governing equations in an elastic medium, consider an infinitesimal surface with normal vector $\hat{\boldsymbol{n}}$ and surface area dS. The traction on this surface is defined by the force acting per unit surface area and is given by

$$\boldsymbol{t}^n = \boldsymbol{\sigma} \cdot \hat{\boldsymbol{n}}, \tag{2.1}$$

where $\boldsymbol{\sigma}$ is the stress tensor and is a crucial quantity to describe the governing equation in an elastic medium since having the stress tensor provides the force acting on any surface using eq. (2.1). Conservation of angular momentum leads to the symmetry property of the stress tensor, thus

$$\sigma_{ij} = \sigma_{ji}. \tag{2.2}$$

In general the stress in a medium depends on the deformation of the medium. The deformation can be defined using the displacement field $\boldsymbol{u}(\boldsymbol{x}, t)$, which varies with position $\boldsymbol{x}$ and time t. In Cartesian tensor notation the displacement is written

$$\boldsymbol{u} = u_i \boldsymbol{e}_{x_i}, \tag{2.3}$$

where (x_1, x_2, x_3) are Cartesian coordinates, $\boldsymbol{e}_{x_i}$ is the unit vector in x_i direction and Einstein's summation convention is used throughout the section so that a repeated index is summed over $i = 1, 2, 3$. The quantity to describe deformation is strain and for small displacements and deformations, the linear strain tensor is defined by

$$\epsilon_{ij} = \frac{1}{2}(\partial_j u_i + \partial_i u_j). \tag{2.4}$$

It is obvious from this definition that the strain tensor is symmetric.

The relation between strain and resulting stress is the constitutive relation which can be linearised for materials experiencing small deformations. Such a linearisation is expressed by Hooke's law and the constitutive relation can be written as

$$\sigma_{ij} = C_{ijkl}\epsilon_{kl}. \tag{2.5}$$

The fourth rank tensor C_{ijkl} is the stiffness tensor which in three dimensions has 81 elements. However, due to symmetry of stress and strain together with energy considerations the stiffness tensor has the following properties

$$C_{ijkl} = C_{jikl} = C_{ijlk} = C_{klij}. \tag{2.6}$$

This reduces the number of independent elements of the fourth rank stiffness tensor to the number of independent elements of a symmetric 6×6 matrix which is 21. Such an analogy facilitates the expression of the stiffness tensor, thus the matrix representation of the stiffness tensor is used wherever convenient. Most natural materials have fewer than 21 independent stiffness components. For an isotropic elastic material the stiffness tensor depends only on the Lamé parameters λ and μ

$$C_{ijkl} = \lambda\delta_{ij}\delta_{kl} + \mu(\delta_{ik}\delta_{jl} + \delta_{il}\delta_{jk}), \tag{2.7}$$

where δ_{ij} is the Kronecker delta. In this section a general stiffness tensor is considered and later on the isotropic case and some examples of other constitutive relations are discussed.

Considering the definition of traction, the force acting on a volume V due to stresses can be calculated by integrating the traction over the surface of the volume S ($\oint \boldsymbol{t}^n \, dS$). Using eq. (2.1) and Gauss theorem it can be shown that the force due to the stress acting on a volume is given by integrating the divergence of the stress tensor over the volume ($\int \partial_i \sigma_{ij} dV$). In addition to this force which is resulting from the deformation of the volume, forces like gravity or other external excitations may act on the volume. These forces are denoted the body forces. Now considering a unit volume Newton's second law can be written as

$$\partial_j \sigma_{ij} + b_i = \rho \ddot{u}_i, \tag{2.8}$$

where $\boldsymbol{b}$ is the body force per unit volume, ρ is the density (mass per unit volume) and $\partial_j \sigma_{ij}$ gives the force acting on a unit volume due to the internal deformation. This is called the wave equation and is the governing equation inside an elastic medium. By considering eqs. (2.4) and (2.5) the governing equation can be written in terms of the displacement field $\boldsymbol{u}$

$$\partial_j (C_{ijkl}\partial_k u_l) + b_i = \rho \ddot{u}_i. \tag{2.9}$$

Considering time harmonic fields with a fixed angular frequency ω, the field variations in time can be expressed as

$$\boldsymbol{u}(\boldsymbol{x}, t) = \mathrm{Re}\left((\boldsymbol{u}(\boldsymbol{x})e^{-i\omega t}\right). \tag{2.10}$$

Such a time harmonic representation simplifies all time derivatives and greatly facilitates the solution of the wave equation. Neglecting the body force, the wave equation simplifies to

$$\partial_j(C_{ijkl}\partial_k u_l) + \rho\omega^2 u_i = 0. \tag{2.11}$$

The wave equation is a second order differential equation for the displacement field $\boldsymbol{u}$. This differential equation needs to be supplemented by some conditions on the boundary of the medium to complete a boundary value problem. In scattering problems the domain of study consists of at least two different parts where the boundary conditions apply to the interface of these domains. This interface may be a closed surface in the case of a bounded domain. By such definition, a wide range of different boundary value problems, like wave propagation in a half space or wave propagation in an infinite medium consisting of a distribution of inclusions, may be considered as a scattering problem. From all these various types of scattering problems, the main interest of this research is the type of problems where an infinite domain, called the matrix, contains at least one finite domain of a different material, called obstacle or scatterer.

One of the main parameters of these scattering problems is the shape of the obstacle. The most common shapes, especially for analytical approaches, are circular shapes like spheres and cylinders in 3D and circles in 2D. The simplicity of these shapes in comparison with more complex ones is crucial for analytical analysis. They are useful to model grainy materials or fiber composites or on a bigger scale buried pipelines, and other practical problems. These types of geometry make it necessary to perform the calculation in curvilinear system of coordinates. Of these the spherical coordinate system is explained in detail in section 2.3.

The other main parameter is the material properties of the matrix and obstacle. The simplest cases are those with all the material properties being isotropic. However, plenty of synthetic and natural materials are not isotropic and this makes it necessary to study cases with anisotropic materials. Some more common types of anisotropy, which are particularly relevant for this study, are explained in section 2.2.

Another important parameter is the number of obstacles. The simplest case is when there is a single obstacle in the matrix. Such problems are briefly explained for isotropic and anisotropic obstacles in chapter 3, and a detailed discussion for anisotropic ones is presented in Papers A-D. In cases involving multiple obstacles, the focus is primarily on scenarios with a random distribution of a large number of obstacles. Various analytical models to handle such a medium are explained in detail in chapter 4.

2.2 Anisotropy of solids

As shown in eq. (2.6) the stiffness tensor which describes the material properties may have 21 independent elements. In most cases the material behaves similarly in some directions and consequently this number of elements is reduced. The simplest case is when the material behaviour is similar in all directions. These are called isotropic materials and the number of independent elements are reduced to two. The independent elements are the Lamé parameters λ and μ. In this case the equation of motion can be simplified to

$$(\lambda + 2\mu)\nabla(\nabla \cdot \boldsymbol{u}) - \mu\nabla \times (\nabla \times \boldsymbol{u}) = -\rho\omega^2\boldsymbol{u}. \tag{2.12}$$

For such a partial differential equation, Helmholtz decomposition is useful for the analysis. The Helmholtz decomposition for an arbitrary vector field like $\boldsymbol{u}$ is

$$\boldsymbol{u} = \nabla\Phi + \nabla \times \boldsymbol{\Psi}, \tag{2.13}$$

where Φ and $\boldsymbol{\Psi}$ are scalar and vector potentials, respectively. Substituting eq. (2.13) into the wave equation eq. (2.12) shows that the potentials should satisfy a Helmholtz equation

$$\begin{aligned} \nabla^2\Phi + k_p^2\Phi &= 0, \\ \nabla^2\boldsymbol{\Psi} + k_s^2\boldsymbol{\Psi} &= 0, \end{aligned} \tag{2.14}$$

where $k_p = \omega\sqrt{\rho/(\lambda + 2\mu)}$ and $k_s = \omega\sqrt{\rho/\mu}$. This shows that there are two types of waves propagating in the medium. One is the wave corresponding to the scalar potential $\boldsymbol{u} = \nabla\Phi$ which is a compressional wave and propagates with the wave number k_p. It can be observed that this wave is irrotational ($\nabla \times \boldsymbol{u} = 0$) and the displacement vector and propagation direction are aligned for a plane wave. Therefore, it is called a longitudinal wave and is often denoted a P wave. The other type of wave is corresponding to the vector potential $\boldsymbol{u} = \nabla \times \boldsymbol{\Psi}$ which is a shear wave and propagates with the wave number k_s. It can be observed that this wave is equivoluminal ($\nabla \cdot \boldsymbol{u} = 0$) and the displacement vector and propagation direction are perpendicular to each other for a plane wave. This wave is called a transverse wave and is often denoted an S wave.

Using eq. (2.13) three quantities u_i are related to four new dependent variables Φ and Ψ_i. Therefore, obviously one degree of arbitrariness is left unspecified for Φ and $\boldsymbol{\Psi}$ potentials. A simple and useful additional restriction on the potentials is to take the vector potential $\boldsymbol{\Psi}$ as divergence free i.e. $\nabla \cdot \boldsymbol{\Psi} = 0$. However, other types of restrictions are considered in the literature, especially to facilitate the solution of the vector potential by uncoupling some components of the fields in curvilinear coordinates. Such restrictions and the solution of scalar and vector potentials in spherical coordinates are discussed in chapter 3.

Besides the isotropic case two special cases of an orthotropic material, which have plenty of applications, is mentioned here. An orthotropic material is characterized by three mutually orthogonal symmetry planes. Thus the number of stiffness constants for an orthotropic material are reduced to nine. The constitutive relations for such a material in matrix notation are

$$\begin{Bmatrix} \sigma_{xx} \\ \sigma_{yy} \\ \sigma_{zz} \\ \sigma_{yz} \\ \sigma_{zx} \\ \sigma_{xy} \end{Bmatrix} = \begin{bmatrix} C_{11} & C_{12} & C_{13} & 0 & 0 & 0 \\ C_{12} & C_{22} & C_{23} & 0 & 0 & 0 \\ C_{13} & C_{23} & C_{33} & 0 & 0 & 0 \\ 0 & 0 & 0 & 2C_{44} & 0 & 0 \\ 0 & 0 & 0 & 0 & 2C_{55} & 0 \\ 0 & 0 & 0 & 0 & 0 & 2C_{66} \end{bmatrix} \begin{Bmatrix} \epsilon_{xx} \\ \epsilon_{yy} \\ \epsilon_{zz} \\ \epsilon_{yz} \\ \epsilon_{zx} \\ \epsilon_{xy} \end{Bmatrix}. \tag{2.15}$$

This is the stress-strain relation of a general orthotropic material. A special case is a cubic material where the material stiffness in all the three coordinate directions are equivalent so the material has three independent stiffness constants and the extra relations among the stiffness components of a general orthotropic material are

$$\begin{aligned} C_{11} &= C_{22} = C_{33}, \\ C_{12} &= C_{13} = C_{23}, \\ C_{44} &= C_{55} = C_{66}. \end{aligned} \tag{2.16}$$

Another special case is a transversely isotropic material. The stiffness for such materials are equal in all directions in a plane which is called the isotropic plane. Consequently the number of independent constants in a transversely isotropic material is five. Taking the xy plane as the isotropic plane the extra relations among the stiffness constants of a general orthotropic material are

$$\begin{aligned} C_{11} &= C_{22}, \\ C_{13} &= C_{23}, \\ C_{44} &= C_{55}, \\ 2C_{66} &= C_{11} - C_{12}. \end{aligned} \tag{2.17}$$

In Paper A and Paper B the material properties of the obstacle (or obstacles) are assumed to be transversely isotropic. Paper C focuses on materials with cubic properties, while Paper D investigates general orthotropic materials.

2.3 Spherical waves

In many scattering problems it is convenient to use curvilinear system of coordinates. Here spherical coordinates are defined and general solutions of the wave equation (wave functions) in this system of coordinates are given.

For the spherical coordinates (r, θ, φ) the relations with Cartesian coordinates (x, y, z) are

$$x = r \sin\theta \cos\varphi, \quad y = r \sin\theta \sin\varphi, \quad z = r \cos\theta. \tag{2.18}$$

The strain displacement relations are

$$
\begin{aligned}
\epsilon_{rr} &= \frac{\partial u_r}{\partial r}, \quad \epsilon_{\varphi\varphi} = \frac{1}{r\sin\theta}\frac{\partial u_\varphi}{\partial \varphi} + \frac{\cot\theta}{r}u_\theta + \frac{u_r}{r}, \\
\epsilon_{\theta\theta} &= \frac{1}{r}\frac{\partial u_\theta}{\partial \theta} + \frac{u_r}{r}, \quad \epsilon_{\theta\varphi} = \frac{1}{2r}\left(\frac{\partial u_\varphi}{\partial \theta} - \cot\theta u_\varphi + \frac{1}{\sin\theta}\frac{\partial u_\theta}{\partial \varphi}\right), \\
\epsilon_{\varphi r} &= \frac{1}{2}\left(\frac{1}{r\sin\theta}\frac{\partial u_r}{\partial \varphi} + \frac{\partial u_\varphi}{\partial r} - \frac{u_\varphi}{r}\right), \quad \epsilon_{r\theta} = \frac{1}{2}\left(\frac{\partial u_\theta}{\partial r} - \frac{u_\theta}{r} + \frac{1}{r}\frac{\partial u_r}{\partial \theta}\right),
\end{aligned}
\tag{2.19}
$$

and the equations of motion in terms of the stresses in this system of coordinates are

$$
\begin{aligned}
&\frac{\partial \sigma_{rr}}{\partial r} + \frac{1}{r}\frac{\partial \sigma_{r\theta}}{\partial \theta} + \frac{1}{r\sin\theta}\frac{\partial \sigma_{r\varphi}}{\partial \varphi} + \frac{1}{r}\left(2\sigma_{rr} - \sigma_{\theta\theta} - \sigma_{r\varphi} + \cot\theta\sigma_{r\theta}\right) - \rho\frac{\partial^2 u_r}{\partial t^2} = 0, \\
&\frac{\partial \sigma_{r\theta}}{\partial r} + \frac{1}{r}\frac{\partial \sigma_{\theta\theta}}{\partial \theta} + \frac{1}{r\sin\theta}\frac{\partial \sigma_{\theta\varphi}}{\partial \varphi} + \frac{1}{r}\left(\cot\theta\left(\sigma_{\theta\theta} - \sigma_{\varphi\varphi}\right) + 3\sigma_{r\theta}\right) - \rho\frac{\partial^2 u_\theta}{\partial t^2} = 0, \\
&\frac{\partial \sigma_{r\varphi}}{\partial r} + \frac{1}{r}\frac{\partial \sigma_{\theta\varphi}}{\partial \theta} + \frac{1}{r\sin\theta}\frac{\partial \sigma_{\varphi\varphi}}{\partial \varphi} + \frac{1}{r}\left(3\sigma_{r\varphi} + 2\cot\theta\sigma_{\theta\varphi}\right) - \rho\frac{\partial^2 u_\varphi}{\partial t^2} = 0.
\end{aligned}
\tag{2.20}
$$

The constitutive relations may be transformed from the Cartesian to the spherical coordinates using the appropriate transformation matrix which is discussed in section 3.1. However, for an isotropic medium the constitutive relations are similar in the spherical and the Cartesian coordinate systems

$$
\begin{Bmatrix} \sigma_{rr} \\ \sigma_{\theta\theta} \\ \sigma_{\varphi\varphi} \\ \sigma_{\theta\varphi} \\ \sigma_{\varphi r} \\ \sigma_{r\theta} \end{Bmatrix} = \begin{bmatrix} \lambda+2\mu & \lambda & \lambda & 0 & 0 & 0 \\ \lambda & \lambda+2\mu & \lambda & 0 & 0 & 0 \\ \lambda & \lambda & \lambda+2\mu & 0 & 0 & 0 \\ 0 & 0 & 0 & 2\mu & 0 & 0 \\ 0 & 0 & 0 & 0 & 2\mu & 0 \\ 0 & 0 & 0 & 0 & 0 & 2\mu \end{bmatrix} \begin{Bmatrix} \epsilon_{rr} \\ \epsilon_{\theta\theta} \\ \epsilon_{\varphi\varphi} \\ \epsilon_{\theta\varphi} \\ \epsilon_{\varphi r} \\ \epsilon_{r\theta} \end{Bmatrix}. \tag{2.21}
$$

Substituting eq. (2.21) into eq. (2.20) gives the equations of motion in terms of the displacements for an isotropic medium. This system of equations may be decomposed into three scalar potentials as [3]

$$
\boldsymbol{u}(\boldsymbol{r}) = \nabla\Phi + \nabla\times(\boldsymbol{r}\Psi_1) + \nabla\times\nabla\times(\boldsymbol{r}\Psi_2), \tag{2.22}
$$

where Φ, Ψ_1 and Ψ_2 are potentials associated to P, SH and SV waves, respectively. These potentials satisfy Helmholtz equations with wavenumbers k_p for Φ and k_s for Ψ_1 and Ψ_2.

Using separation of variables to solve the scalar Helmholtz equations in spherical coordinates leads to trigonometric functions $\cos m\varphi$ or $\sin m\varphi$, where $m = 0, 1, 2, ...$ for the azimuthal factor (φ), associated Legendre functions with $\cos\theta$ argument as $P_l^m(\cos\theta)$ with $l = m, m+1, m+2, ...$ for the polar factor (θ) and spherical Bessel j_m or Hankel $h_m^{(1)}$ functions for the radial factor (r), and the potentials may be written as

$$
\begin{aligned}
\Phi^0 &= j_m(k_p r)Y_{\sigma ml}(\theta,\varphi), \\
\Psi_1^0 &= j_m(k_s r)Y_{\sigma ml}(\theta,\varphi), \\
\Psi_2^0 &= j_m(k_s r)Y_{\sigma ml}(\theta,\varphi).
\end{aligned}
\tag{2.23}
$$

The upper index 0 denotes that they are regular waves, containing spherical Bessel functions j_m, and the corresponding outgoing waves denoted by + contain spherical Hankel functions $h_m^{(1)}$. The $Y_{\sigma ml}(\theta,\varphi)$ are called spherical harmonics with the following definition

$$Y_{\sigma ml}(\theta,\varphi) = \sqrt{\frac{\epsilon_m(2l+1)(l-m)!}{4\pi(l+m)!}} P_l^m(\cos\theta) \left\{ \begin{array}{c} \cos m\varphi \\ \sin m\varphi \end{array} \right\}, \tag{2.24}$$

where $\sigma = e$ is for the upper row which is even with respect to φ and $\sigma = o$ is for the lower row which is odd with respect to φ. Indices l and m run through $m = 0, 1, 2, ...$ and $l = m, m+1, m+2, ...$ The Neumann factor $\epsilon_0 = 1$ and $\epsilon_m = 2$ for $m = 1, 2, ...$ The spherical harmonics constitute a complete orthonormal set on the unit sphere.

Thus the general solution for the displacement field may be written in terms of the spherical vector wave functions which are defined as

$$\begin{aligned}
\boldsymbol{\psi}^0_{1\sigma ml}(r,\theta,\varphi) &= \frac{1}{\sqrt{l(l+1)}} \nabla \times \left(\boldsymbol{r}\Psi_1^0 \right) = j_l(k_s r) \boldsymbol{A}_{1\sigma ml}(\theta,\varphi), \\
\boldsymbol{\psi}^0_{2\sigma ml}(r,\theta,\varphi) &= \frac{1}{\sqrt{l(l+1)}} \frac{1}{k_s} \nabla \times \nabla \times \left(\boldsymbol{r}\Psi_2^0 \right) \\
&= \left(j_l'(k_s r) + \frac{j_l(k_s r)}{k_s r} \right) \boldsymbol{A}_{2\sigma ml}(\theta,\varphi) + \sqrt{l(l+1)} \frac{j_l(k_s r)}{k_s r} \boldsymbol{A}_{3\sigma ml}(\theta,\varphi), \\
\boldsymbol{\psi}^0_{3\sigma ml}(r,\theta,\varphi) &= \left(\frac{k_p}{k_s} \right)^{3/2} \frac{1}{k_p} \nabla \left(\Phi^0 \right) \\
&= \left(\frac{k_p}{k_s} \right)^{3/2} \left((j_l'(k_p r) \boldsymbol{A}_{3\sigma ml}(\theta,\varphi) + \sqrt{l(l+1)} \frac{j_l(k_p r)}{k_p r} \boldsymbol{A}_{2\sigma ml}(\theta,\varphi) \right),
\end{aligned} \tag{2.25}$$

where the first index is denoted $\tau = 1, 2, 3$ for SH, SV and P wave function, respectively. Here again, the upper index 0 denotes that they are regular vector wave functions and the corresponding outgoing wave functions denoted by + contain spherical Hankel functions $h_m^{(1)}$. $\boldsymbol{A}_{\tau\sigma ml}$ are the vector spherical harmonics which are defined as

$$\begin{aligned}
\boldsymbol{A}_{1\sigma ml}(\theta,\varphi) &= \frac{1}{\sqrt{l(l+1)}} \nabla \times (\boldsymbol{r} Y_{\sigma ml}(\theta,\varphi)) \\
&= \frac{1}{\sqrt{l(l+1)}} \left(\boldsymbol{e}_\theta \frac{1}{\sin\theta} \frac{\partial}{\partial\varphi} Y_{\sigma ml}(\theta,\varphi) - \boldsymbol{e}_\varphi \frac{\partial}{\partial\theta} Y_{\sigma ml}(\theta,\varphi) \right), \\
\boldsymbol{A}_{2\sigma ml}(\theta,\varphi) &= \frac{1}{\sqrt{l(l+1)}} r \nabla Y_{\sigma ml}(\theta,\varphi) \\
&= \frac{1}{\sqrt{l(l+1)}} \left(\boldsymbol{e}_\theta \frac{\partial}{\partial\theta} Y_{\sigma ml}(\theta,\varphi) + \boldsymbol{e}_\varphi \frac{1}{\sin\theta} \frac{\partial}{\partial\varphi} Y_{\sigma ml}(\theta,\varphi) \right), \\
\boldsymbol{A}_{3\sigma ml}(\theta,\varphi) &= \boldsymbol{e}_r Y_{\sigma ml}(\theta,\varphi).
\end{aligned} \tag{2.26}$$

The spherical vector wave functions provide a comprehensive representation of the wave behavior in isotropic materials within the spherical coordinate system. In the following section, solving scattering problems is discussed with the means of concepts and quantities described here.

3 Scattering Problems

The focus of this study is on scattering by spherical obstacles surrounded by an isotropic medium. It is then convenient to express the displacement field in the surrounding medium as a sum of the incident wave $\boldsymbol{u}^{in}$ (corresponds to the regular wave) and the wave scattered by the obstacle $\boldsymbol{u}^{sc}$ (corresponds to the outgoing wave). Using the vector spherical wave function of eq. (2.25) the displacement field in the surrounding medium is

$$\boldsymbol{u}(\boldsymbol{r}) = \boldsymbol{u}^{in} + \boldsymbol{u}^{sc} = \sum_{\tau\sigma ml} (a_{\tau\sigma ml}\boldsymbol{\psi}^0_{\tau\sigma ml}(\boldsymbol{r}) + b_{\tau\sigma ml}\boldsymbol{\psi}^+_{\tau\sigma ml}(\boldsymbol{r})). \tag{3.1}$$

As the underlying problem is linear, it is possible to write [31]

$$b_{\tau\sigma ml} = \sum_{\tau'\sigma'm'l'} T_{\tau\sigma ml,\tau'\sigma'm'l'} a_{\tau'\sigma'm'l'}, \tag{3.2}$$

where $\mathbf{T}$ is a an infinite matrix called the transition matrix. The transition matrix characterizes the scattering properties of the obstacle and provides information about how the obstacle scatters the incident wave and interacts with its surroundings. It is a matrix that depends on various factors such as the shape of the obstacle, the boundary conditions, the elastic properties of the material, and the frequency of excitation. Importantly, the transition matrix is independent of the incident field, which makes it a valuable building block for tackling more complex problems involving multiple obstacles.

The $\mathbf{T}$ matrix elements are typically determined by applying boundary conditions. In the case of a spherical obstacle, the boundary of the sphere with radius a can be defined by setting $r = a$ in a spherical coordinate system centered at the center of the sphere. Additionally, for perfectly welded boundary conditions, the displacement and traction fields must be continuous at the boundary which means

$$\begin{aligned} \boldsymbol{u}(\boldsymbol{a}) &= \boldsymbol{u}_1(\boldsymbol{a}), \\ \boldsymbol{t}^{(r)}(\boldsymbol{a}) &= \boldsymbol{t}_1^{(r)}(\boldsymbol{a}), \end{aligned} \tag{3.3}$$

where $\boldsymbol{t}^{(r)}$ represents the traction in the radial direction, and the subscript 1 denotes the fields and quantities inside the sphere. The radial traction for an isotropic medium can be expressed in terms of the displacement field as

$$\boldsymbol{t}^{(r)} = \boldsymbol{e}_r \lambda \nabla \cdot \boldsymbol{u} + \mu\left(2\frac{\partial \boldsymbol{u}}{\partial r} + \boldsymbol{e}_r \times (\nabla \times \boldsymbol{u})\right). \tag{3.4}$$

With this relation, the radial traction for each spherical vector wave function can be calculated as

$$
\begin{aligned}
\boldsymbol{t}^{(r)}\left(\boldsymbol{\psi}^0_{1\sigma ml}(\boldsymbol{r})\right) &= \mu r \frac{d}{dr}\left(\frac{j_l(k_s r)}{r}\right)\boldsymbol{A}_{1\sigma ml}(\theta,\varphi), \\
\boldsymbol{t}^{(r)}\left(\boldsymbol{\psi}^0_{2\sigma ml}(\boldsymbol{r})\right) &= \mu \left[2\sqrt{l(l+1)}\frac{d}{dr}\left(\frac{j_l(k_s r)}{k_s r}\right)\boldsymbol{A}_{3\sigma ml}(\theta,\varphi) \right. \\
&\quad \left. + \left(2k_s j_l''(k_s r) + \frac{2j_l'(k_s r)}{r} - \frac{2j_l(k_s r)}{k_s r^2} + k_s j_l(k_s r)\right)\boldsymbol{A}_{2\sigma ml}(\theta,\varphi)\right], \\
\boldsymbol{t}^{(r)}\left(\boldsymbol{\psi}^0_{3\sigma ml}(\boldsymbol{r})\right) &= \mu\left(\frac{k_p}{k_s}\right)^{3/2}\left[\left(2k_p j_l''(k_p r) + \frac{2k_p^2 - k_s^2}{k_p} j_l(k_p r)\right)\boldsymbol{A}_{3\sigma ml}(\theta,\varphi)\right. \\
&\quad \left. + 2\sqrt{l(l+1)}\frac{d}{dr}\left(\frac{j_l(k_p r)}{k_p r}\right)\boldsymbol{A}_{2\sigma ml}(\theta,\varphi)\right].
\end{aligned} \tag{3.5}
$$

In the case of an isotropic sphere the displacement and traction fields inside the sphere can be expanded in the regular spherical vector wave functions

$$\boldsymbol{u}_1(\boldsymbol{r}) = \sum_{\tau\sigma ml} c_{\tau\sigma ml}\boldsymbol{\psi}^0_{\tau\sigma ml,1}(\boldsymbol{r}), \tag{3.6}$$

$$\boldsymbol{t}^{(r)}_1(\boldsymbol{r}) = \sum_{\tau\sigma ml} c_{\tau\sigma ml}\boldsymbol{t}^{(r)}\left(\boldsymbol{\psi}^0_{\tau\sigma ml,1}(\boldsymbol{r})\right), \tag{3.7}$$

where $c_{\tau\sigma ml}$ are the unknown coefficients inside the sphere yet to be determined and $\boldsymbol{\psi}^0_{\tau\sigma ml,1}$ are the spherical vector wave functions of the elastic medium inside the sphere.

The spherical vector wave functions are expressed in terms of the orthogonal vector spherical harmonics. As a result, the boundary conditions given in eq. (3.3) decouple for each order of σ, m, and l. Furthermore, the spherical vector wave function for $\tau = 1$ depends only on $\boldsymbol{A}_{1\sigma ml}$ and is decoupled from the vector wave functions of $\tau = 2$ and $\tau = 3$, which both depend on $\boldsymbol{A}_{2\sigma ml}$ and $\boldsymbol{A}_{3\sigma ml}$ and are coupled. Essentially, for each partial wave of order τ, σ, m, and l, there are two unknown coefficients, $c_{\tau\sigma ml}$ and $b_{\tau\sigma ml}$, and two equations from the continuity of the displacement and traction fields. This provides sufficient information to determine the unknowns and find the $\mathbf{T}$ matrix elements. This problem has been extensively discussed in the literature [3].

When the sphere is anisotropic, the classical solution in terms of the spherical vector wave functions inside the sphere is not directly applicable, which adds complexity to the problem. The main objective of this study is to broaden the range of possible analytical solutions to include also the scattering of elastic waves by an anisotropic sphere. In the upcoming section, the methodology employed to address this problem is briefly outlined, followed by the simplest possible example, namely the scattering of a torsional (scalar) wave by an anisotropic sphere in an axisymmetric setting.

3.1 Scattering by an anisotropic sphere

To solve the problem of scattering by an anisotropic sphere a series expansion approach is adopted. As the surrounding medium is isotropic, the displacement and traction field outside the sphere are expanded as stated in eqs. (3.1) and (3.4). For the fields inside the anisotropic sphere such expressions are not valid. In this case, the vector spherical harmonics can serve as bases for the $\theta\varphi$ dependence. As a result, any vector valued function, including the displacement field, can be expressed as a sum of vector spherical harmonics

$$\boldsymbol{u}_1(r,\theta,\varphi) = \sum_{\tau\sigma ml} F_{\tau\sigma ml}(r)\boldsymbol{A}_{\tau\sigma ml}(\theta,\varphi), \tag{3.8}$$

where $l = 1, 2, \ldots$ for $\tau = 1, 2$ and $l = 0, 1, \ldots$ for $\tau = 3$. Such expansions facilitate the application of the boundary conditions as the fields outside the sphere are also in terms of the vector spherical harmonics. Considering the regularity condition at the center of the sphere, the r dependent coefficients $F_{\tau\sigma ml}(r)$ are expanded in power series in r as

$$\begin{aligned}
F_{1\sigma ml}(r) &= \sum_{j=l,l+2,\ldots}^{\infty} f_{1\sigma ml,j}r^j, \\
F_{2\sigma ml}(r) &= \sum_{j=l-1,l+1,\ldots}^{\infty} f_{2\sigma ml,j}r^j, \\
F_{3\sigma ml}(r) &= \sum_{j=l-1,l+1,\ldots}^{\infty} f_{3\sigma ml,j}r^j,
\end{aligned} \tag{3.9}$$

in which $f_{3\sigma m0,-1} = 0$. Here, $f_{\tau\sigma ml,j}$ are the unknown coefficients inside the sphere.

The radial traction inside the sphere can be calculated using the constitutive relation based on the material properties. In the case where the sphere has anisotropic properties in Cartesian coordinates, as explained in section 2.2, the starting point is to establish the stress-strain relations in spherical coordinates. This is achieved by transforming the constitutive relations from Cartesian coordinates to spherical coordinates. To do so, the following relation for the transformation of a second rank tensor like stress and strain from the Cartesian to the spherical coordinates is used

$$\mathbf{S}_s = \mathbf{R}^T\mathbf{S}_c\mathbf{R}, \tag{3.10}$$

where $\mathbf{S}_s$ and $\mathbf{S}_c$ are second rank tensors in the spherical and the Cartesian coordinates, respectively, and $\mathbf{R}$ is the rotation matrix with the following appearance

$$\mathbf{R} = \begin{bmatrix} \cos\varphi\sin\theta & \cos\varphi\cos\theta & -\sin\varphi \\ \sin\varphi\sin\theta & \sin\varphi\cos\theta & \cos\varphi \\ \cos\theta & -\sin\theta & 0 \end{bmatrix}. \tag{3.11}$$

Using the spherical strain relations as described in eq. (2.19), it is possible to express the radial traction in terms of the displacement field in spherical coordinates. This provides the necessary relations to apply boundary conditions. However, there are two challenges in solving the problem. First, after the transformation, the traction field consists of terms involving multiplication of trigonometric functions and vector spherical harmonics. This can make it difficult to directly apply boundary conditions due to the complexity of these terms. Second, the unknown coefficients inside the sphere for each order of τ, σ, m, and l are more than one, as determined by the power series expansion in the radial direction eq. (3.9). Consequently, the number of unknowns exceeds the number of equations imposed by the boundary conditions.

To address the first challenge, the orthogonality of the vector spherical harmonics is used. Therefore, the traction field at the boundary $r = a$ can be expanded as

$$\boldsymbol{t}_1^{(r)}(a, \theta, \varphi) = \sum_{\tau\sigma ml} G_{\tau\sigma ml}(a) \boldsymbol{A}_{\tau\sigma ml}(\theta, \varphi), \tag{3.12}$$

where the coefficients $G_{\tau\sigma ml}$ can be found using the scalar product of the traction field and vector spherical harmonics

$$G_{\tau\sigma ml}(a) = \int_S \boldsymbol{t}_1^{(r)}(a, \theta, \varphi) \cdot \boldsymbol{A}_{\tau\sigma ml}(\theta, \varphi) dS. \tag{3.13}$$

Here S is the unit sphere. Once the displacement and traction field expansions are given as eqs. (3.8) and (3.12), the application of boundary conditions becomes straightforward.

The scattering problem remains unsolved due to the higher number of unknowns compared to the available boundary condition equations. To address this, it is necessary for the fields inside the sphere to satisfy the governing equations within the sphere (eq. (2.20)). Consequently, by substituting the stress relations into the governing equations, a system of equations among the unknown coefficients inside the sphere is obtained. To facilitate the analysis, it is advantageous to express the governing equations in terms of orthogonal functions in angular directions. Using again the vector spherical harmonics, it is possible to express the governing equations as

$$\sum_{\tau\sigma ml} H_{\tau\sigma ml}(r) \boldsymbol{A}_{\tau\sigma ml}(\theta, \varphi) = \mathbf{0}, \tag{3.14}$$

where $H_{\tau\sigma ml}$ may be found using the same procedure as for $G_{\tau\sigma ml}$. The orthogonality of the vector spherical harmonics forces all these coefficients, which are power series in r, to vanish so that

$$H_{\tau\sigma ml}(r) = 0 \qquad \text{for all} \quad \tau, \sigma, m, l. \tag{3.15}$$

Since the powers of r are linearly independent, it is necessary for the coefficient in front of each power of r to vanish. This condition gives rise to recursion relations among the unknown coefficients inside the sphere, resulting in that only one unknown remains for each partial wave. These recursion relations reveal the coupling between different partial waves, which is fundamentally influenced by the symmetry of anisotropy.

The recursion relation described in eq. (3.15), along with the series expansion of the displacement and traction fields inside the sphere, provides the necessary framework to solve the scattering problem. By substituting these expansions into the governing equations and applying the boundary conditions stated in eq. (3.3), the system of equations involving the unknown coefficients can be solved. This process allows for the determination of the **T** matrix element.

The approach described above is initially presented in Paper A, where the focus is on an axisymmetric problem. This particular case is discussed briefly in the following section. Subsequently, Papers B-D explore the general problem for various classes of anisotropy. Each anisotropy class exhibits different coupling effects among the partial waves, which are determined by the symmetry planes of the respective class. More detailed explanations of these phenomena can be found in the appended papers.

3.2 Torsional (scalar) scattering by a TI sphere

In this section, the general problem described in section 3.1 is simplified to a scalar and axisymmetric one. This can be achieved by considering a transversely isotropic sphere with the axis of anisotropy perpendicular to the xy plane, and an incident plane torsional wave parallel to the axis of anisotropy (z axis). Such a rotationally symmetric incident wave together with symmetrical geometry and material properties lead to φ independent displacement and stress fields. As a result, the sum over vector wave functions only includes terms with $m = 0$ and $\sigma = e$. Furthermore, considering that the incident wave is polarized only in the φ direction (a torsional wave), the problem reduces to a scalar one, relating solely to the motion in the azimuthal φ direction.

With these assumptions, the incident and scattered wave displacement and traction fields of the surrounding medium from eq. (3.1) and eq. (3.5) are reduced to the case with $\tau = 1, m = 0$ and $\sigma = e$ as

$$u_{\varphi}^{in}(r,\theta) = \sum_{l=1}^{\infty} a_l \boldsymbol{\psi}_{1e0l}^{0}(r,\theta) \cdot \boldsymbol{e}_{\varphi} = \sum_{l=1}^{\infty} a_l w_l j_l(k_s r) P_l^1(\cos\theta), \tag{3.16}$$

$$u_{\varphi}^{sc}(r,\theta) = \sum_{l=1}^{\infty} b_l \boldsymbol{\psi}_{1e0l}^{+}(r,\theta) \cdot \boldsymbol{e}_{\varphi} = \sum_{l=1}^{\infty} b_l w_l h_l^{(1)}(k_s r) P_l^1(\cos\theta), \tag{3.17}$$

$$\sigma_{r\varphi}^{in} = \sum_{l=1}^{\infty} a_{1l} \mu r w_l \frac{d}{dr}\left(\frac{j_l(k_s r)}{r}\right) P_l^1(\cos\theta), \tag{3.18}$$

$$\sigma_{r\varphi}^{sc} = \sum_{l=1}^{\infty} b_{1l} \mu r w_l \frac{d}{dr}\left(\frac{h_l^{(1)}(k_s r)}{r}\right) P_l^1(\cos\theta), \tag{3.19}$$

where $w_l = \sqrt{(2l+1)/(4\pi l(l+1))}$. In this section, the indices $\tau = 1$, $m = 0$, and $\sigma = e$ are omitted for brevity. As a result, the notation $\boldsymbol{A}_{1e0l}(\theta)$ simplifies to $\boldsymbol{A}_l(\theta)$.

Furthermore, since $\boldsymbol{A}_l(\theta)$ only depends on the associated Legendre function of order 1, denoted as $P_l^1(\cos\theta)$, this function is used in place of $\boldsymbol{A}_l(\theta)$ throughout this section. The **T** matrix then is simplified to

$$b_l = \sum_{l'=1}^{\infty} T_{l,l'} a_{l'}. \tag{3.20}$$

Inside the sphere the governing equation becomes

$$\frac{\partial \sigma_{r\varphi}}{\partial r} + \frac{1}{r}\frac{\partial \sigma_{\theta\varphi}}{\partial \theta} + \frac{1}{r}\left(3\sigma_{r\varphi} + 2\cot\theta\sigma_{\theta\varphi}\right) + \rho\omega^2 u_\varphi = 0. \tag{3.21}$$

The stress-strain relations in spherical coordinates are derived from the transformation of the constitutive relation for a transversely isotropic medium (eqs. (2.15) and (2.17)) from Cartesian to spherical coordinates according to eq. (3.10). In the specific problem at hand, the non-zero stress relations are

$$\sigma_{r\varphi} = \alpha\epsilon_{r\varphi} - \beta\left(\epsilon_{r\varphi}\cos 2\theta - \epsilon_{\theta\varphi}\sin 2\theta\right), \tag{3.22}$$

$$\sigma_{\theta\varphi} = \alpha\epsilon_{\theta\varphi} + \beta\left(\epsilon_{\theta\varphi}\cos 2\theta + \epsilon_{r\varphi}\sin 2\theta\right), \tag{3.23}$$

where $\alpha = \frac{1}{2}(C_{11} - C_{12} + 2C_{44})$ and $\beta = \frac{1}{2}(C_{11} - C_{12} - 2C_{44})$. In the isotropic limit $\alpha = 2\mu_1$ (μ_1 being the Lamé parameter of the sphere), and $\beta = 0$ which eliminates all the terms with trigonometric functions.

Considering the fields inside the sphere and the orthogonality of the associated Legendre functions, the displacement field is expanded in the θ direction as

$$u_\varphi(r,\theta) = \sum_{l=1}^{\infty} F_l(r) P_l^1(\cos\theta). \tag{3.24}$$

The function $F_l(r)$ can be expanded according to eq. (3.9)

$$F_l(r) = \sum_{j=l,l+2,\ldots} f_{j,l} r^j. \tag{3.25}$$

Substituting such an expansion of the displacement field into the radial traction (eq. (3.22)) and the governing equation (eq. (3.21)) leads to

$$\begin{aligned}\sigma_{r\varphi} = \frac{\alpha}{2}\sum_{l=1}^{\infty}&(1+\bar{\beta})(F_l'(r) - \frac{F_l(r)}{r})P_l^1(\cos\theta) - 2\bar{\beta}\cos^2\theta P_l^1(\cos\theta)F_l'(r) \\ &- 2\bar{\beta}\frac{dP_l^1(\cos\theta)}{d\cos\theta}\sin^2\theta\cos\theta(\frac{F_l(r)}{r}),\end{aligned} \tag{3.26}$$

$$
\begin{aligned}
&\sum_{l=1}^{\infty}\Bigg[P_l^1(\cos\theta)\Bigg[(1+\bar{\beta})F_l''(r)+\frac{2}{r}F_l'(r)-\Big(l(l+1)+\bar{\beta}\big(2-l(l+1)\big)\Big)\frac{1}{r^2}F_l(r)\Bigg]\\
&\quad+P_l^1(\cos\theta)\cos^2\theta\Bigg[2\bar{\beta}\big(-F_l''(r)+\frac{1}{r}F_l'(r)-l(l+1)\frac{1}{r^2}F_l(r)\big)\Bigg]\\
&\quad+\frac{dP_l^1(\cos\theta)}{d\cos\theta}\sin^2\theta\cos\theta\Bigg[2\bar{\beta}(-\frac{2}{r}F_l'(r)+\frac{1}{r^2}F_l(r))\Bigg]+k^2F_l(r)P_l^1(\cos\theta)\Bigg]=0,
\end{aligned}
\tag{3.27}
$$

where $\bar{\beta}=\beta/\alpha$ and $k=\omega\sqrt{2\rho_1/\alpha}$.

As discussed in the previous section these functions may be expanded in terms of the associated Legendre functions $P_l^1(\cos\theta)$ as

$$
\sigma_{r,\varphi}(r)=\frac{\alpha}{2}\sum_l G_l(r)P_l^1(\cos\theta),
\tag{3.28}
$$

$$
\sum_l H_lP_l^1(\cos\theta)=0.
\tag{3.29}
$$

with

$$
G_l(r)=\sum_{j=l,l+2,\dots}\Big[f_{j,l}N_{1j,l}+f_{j,l+2}N_{2j,l}+f_{j,l-2}N_{3j,l}\Big]r^{j-1},
\tag{3.30}
$$

$$
H_l(r)=\sum_{j=l,l+2,\dots}\Big(f_{j,l}M_{1j,l}+f_{j,l+2}M_{2j,l}+f_{j,l-2}M_{3j,l}+f_{j+2,l}k^2\Big)r^{j-2}.
\tag{3.31}
$$

The coefficients $N_{ij,l}$ and $M_{ij,l}$, where $i=1,2,3$, are functions of l, j, and $\bar{\beta}$. The detailed definition and derivation of these coefficients can be found in Paper A. It is noteworthy that these relations demonstrate coupling among the orders l, $l+2$, and $l-2$, which arises as a consequence of anisotropy in the system. However, in the isotropic limit when $\bar{\beta}=0$, the parameters simplify to $N_{ij,l}=M_{ij,l}=0$ for $i=2$ and 3, and no coupling among different orders remains.

By utilizing the series expansions given in eqs. (3.24) and (3.28) for the fields inside the sphere, and eqs. (3.16) to (3.19) for the fields outside the sphere, the following two equations are obtained for each order of l from the boundary conditions

$$
\sum_{j=l,l+2,\dots} f_{j,l}a^j=a_lw_lj_l(k_sa)+b_lw_lh_l^{(1)}(k_sa),
\tag{3.32}
$$

$$
\begin{aligned}
&\sum_{j=l,l+2,\dots}\alpha\Big(f_{j,l}N_{1j,l}+f_{j,l+2}N_{2j,l}+f_{j,l-2}N_{3j,l}\Big)a^{j-1}=\\
&\qquad 2\mu rw_la_l\frac{d}{dr}\left(\frac{j_l(k_sr)}{r}\right)\Bigg|_{r=a}+2\mu rw_lb_l\frac{d}{dr}\left(\frac{h_l^{(1)}(k_sr)}{r}\right)\Bigg|_{r=a}.
\end{aligned}
\tag{3.33}
$$

Furthermore, the powers of r are linearly independent and eqs. (3.29) and (3.31) yields

$$f_{j,l}M_{1j,l} + f_{j,l+2}M_{2j,l} + f_{j,l-2}M_{3j,l} + f_{j+2,l}k^2 = 0, \tag{3.34}$$

for all $l = 1, 2, ..,$ and $j = l, l+2, ..,$ with the condition $f_{j,l} = 0$ for all $j < l$. This recursion relation can be used to determine all $f_{j,l}$ for $j = l+2, l+4, \ldots$ in terms of $f_{l,l}$, leaving only one unknown inside the sphere for each l. With one unknown outside the sphere b_l, the system of equations eqs. (3.32) and (3.33) is sufficient to solve the problem and find the $\mathbf{T}$ matrix elements. In the low-frequency limit, it is sufficient to study the system only for $l = 1$, and 2 and explicitly derive the leading order elements of the $\mathbf{T}$ matrix as

$$\begin{aligned} T_{11} &= -\frac{ik_s^5a^5}{45}(1 - \frac{\rho_1}{\rho}), \\ T_{22} &= -\frac{ik_s{}^5a^5(C_{44} - \mu)}{45(C_{44} + 4\mu)}. \end{aligned} \tag{3.35}$$

In this case, the leading order $\mathbf{T}$ matrix elements for SH waves are of order k_s^5, which is higher compared to the leading order for P-SV waves, shown to be k_p^3. As a result, SH waves have limited significance in low frequency evaluations. Additionally, T_{11} for $l = 1$ is solely dependent on the density of the sphere, which is reasonable since the $l = 1$ case at low frequencies is associated with the rigid body rotation of the sphere. For $l = 2$, T_{22} is solely dependent on the shear modulus C_{44}.

In this simplified problem, it is possible to derive the system of equations for arbitrary orders of l. However, in the more general problems addressed in Papers B-D, the system of equations is explicitly derived only for the orders of l and m that are relevant for low-frequency studies. For higher orders, numerical methods are employed to solve the problem, as the complexity increases and explicit analytical solutions become hard to derive and less practical.

4 Inhomogeneous Media

In an inhomogeneous medium the physical properties exhibit spatial variations, resulting in complex wave propagation phenomena. This is in contrast to a homogeneous medium, where the physical properties remain uniform and constant throughout. Inhomogeneous media appears in many forms and find applications in fields like geophysics, medical imaging, and material science. In material science, various types of inhomogeneous materials exist, including composite materials composed of multiple phases and polycrystalline materials characterized by a grainy structure of constituent crystals.

Early investigations into inhomogeneous materials focused on cases where the structure of the inhomogeneities followed a periodic pattern or had a deterministic distribution, as seen in laminated and fibrous composite media. However, this assumption overlooked the fact that many materials exhibit inhomogeneities that are random in nature.

The theory of wave propagation in random media focuses on the study of wave behavior in materials with intricate spatial variations in their properties. These variations make it challenging to describe the materials properties deterministically, and instead their properties are characterized statistically. The theory of wave propagation in random media includes two main approaches: the continuous random media, which are referred to as the macroscopic approach by Frisch [32], and the multiple scattering theory which explores the scattering of waves by randomly distributed discrete scatterers and is called the microscopic approach [32]. In the continuous random medium, the medium is approximated by a reference homogeneous medium with a zero-mean fluctuation. The average field inside the medium is then estimated by considering the fluctuation and employing perturbation methods. On the other hand, in the multiple scattering theory, wave propagation in the inhomogeneous medium is analysed based on the scattering properties of individual scatterers.

In this section, first a brief description of the fundamental concepts and assumptions of each of these approaches is presented for simple scalar waves. Then their application in propagation of elastic waves in grainy structured materials such as polycrystalline materials is discussed.

4.1 Multiple scattering

Early studies on multiple scattering include those by Foldy [19], Lax [33], and Snyder and Scott [34] which is developed further by Twersky [35] and Waterman and Truell [36]. It is not within the scope of this study to discuss the physical and mathematical merits of different methods. Instead, only the Foldy theory is considered for the investigation of wave propagation in random inhomogeneous media, and thus its concepts and derivation are discussed in this section. For recent studies and comparison of different multiple scattering theories one can refer to Anson and Chivers [37] and Martin [31]. For simplicity the main concepts are described here for the Helmholtz scalar wave equation as

$$(\nabla^2 + k^2)u^0 = 0, \tag{4.1}$$

where k is the wave number and u^0 is the displacement field in the medium without any scatterer. Supposing the medium include N point scatterers, the propagating field inside the medium satisfies the following equation [19]

$$u(\boldsymbol{r}) = u^0(\boldsymbol{r}) + \sum_{j=1}^{N} T(\boldsymbol{r}_j)u^j(\boldsymbol{r})E(\boldsymbol{r}, \boldsymbol{r}_j), \tag{4.2}$$

where $u(\boldsymbol{r})$ represents the field at point $\boldsymbol{r}$ in the medium, $u^j(\boldsymbol{r})$ is the field acting on the scatterer located at $\boldsymbol{r}_j$, $T(\boldsymbol{r}_j)$ represents the scattering characteristic of the scatterer located at $\boldsymbol{r}_j$, and $E(\boldsymbol{r}, \boldsymbol{r}_j) = \exp(ik|\boldsymbol{r} - \boldsymbol{r}_j|)/|\boldsymbol{r} - \boldsymbol{r}_j|$ represents the far field propagation of the scattered wave in the k medium. The field acting on the jth scatterer is then depending on the scattering of other scatterers and can be expressed as

$$u^j(\boldsymbol{r}) = u^0(\boldsymbol{r}) + \sum_{j'=1, j' \neq j}^{N} T(\boldsymbol{r}_{j'}) u^{j'}(\boldsymbol{r}) E(\boldsymbol{r}, \boldsymbol{r}_{j'}). \tag{4.3}$$

The eqs. (4.2) and (4.3) can be interpreted as describing consecutive scattering processes. The first equation indicates that the field scattered by a scatterer at point $\boldsymbol{r}_j$ depends on the scattering characteristic of the scatterer (T) and the field acting on it (u^j). The second equation indicates that the field action on the scatterer j is equal to the sum of the incident and the scattered field contributed by other scatterers, excluding scatterer j. Equations (4.2) can be iterated any number of times, and each iteration can be related to a specific event of scattering (see fig. 4.1).

Equations (4.2) and (4.3) are useful for understanding the scattering processes involved, but is impractical for the evaluation of the effective quantities when there are large number of scatterers which are randomly distributed throughout the medium. To deal with the randomness, the average field is studied instead. For this purpose, the statistical data of the scatterers are used to evaluate the average of any desired field in the medium.

With a collection of N scatterers, each with distinct scattering characteristics $T(\boldsymbol{r}_j, s_j)$ where the parameter s_j define the state of the scatterer such as shape, size, orientation, and mechanical properties and $\boldsymbol{r}_j$ indicates the location of the scatterer in the spatial domain. The probability of these scatterers existing within the volume elements $d\boldsymbol{r}_1 d\boldsymbol{r}_2 \ldots d\boldsymbol{r}_N$, while their respective states fall within the region $ds_1 ds_2 \ldots ds_N$ can be expressed as [33]

$$P(\boldsymbol{r}_1 \boldsymbol{r}_2 ... \boldsymbol{r}_N; s_1 s_2 ... s_N) d\boldsymbol{r}_1 d\boldsymbol{r}_2 ... d\boldsymbol{r}_N ds_1 ds_2 ... ds_N. \tag{4.4}$$

This quantity is defined in a way that its integral is normalized to unity. With this definition, the probability distribution of a scatterer comes form the integration over all the remaining scatterers

$$P(\boldsymbol{r}_1; s_1) = \int_{V_t} \int P(\boldsymbol{r}_1 \boldsymbol{r}_2 ... \boldsymbol{r}_N; s_1 s_2 ... s_N) d\boldsymbol{r}_2 ... d\boldsymbol{r}_N ds_2 ... ds_N, \tag{4.5}$$

where V_t is the total volume accessible to the scatterers.

Probability distributions are normally converted to density distribution $n(\boldsymbol{r}_1; s_1)$ by considering the total number of scatterers as

$$n(\boldsymbol{r}_1; s_1) = N P(\boldsymbol{r}_1; s_1). \tag{4.6}$$

Assuming that the probability distribution of each scatterer is not influenced by other scatterers, meaning that

$$P(\boldsymbol{r}_1 \boldsymbol{r}_2 ... \boldsymbol{r}_N; s_1 s_2 ... s_N) = P(\boldsymbol{r}_1; s_1) P(\boldsymbol{r}_2; s_2) ... P(\boldsymbol{r}_N; s_N), \tag{4.7}$$

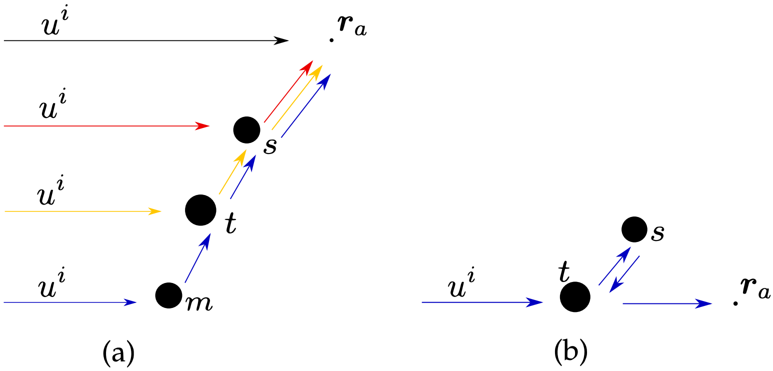

Figure 4.1: (a) Events of scattering going through different scatterers, and (b) events of scattering which a scatterer contributes more than once [38].

the ensemble average of a field is

$$\begin{aligned} < u(\boldsymbol{r}) > = \int_V \int u(\boldsymbol{r}; \boldsymbol{r}_1, \boldsymbol{r}_2 ... \boldsymbol{r}_n; s_1, s_2, s_N) \\ P(\boldsymbol{r}_1; s_1) P(\boldsymbol{r}_2; s_2) ... P(\boldsymbol{r}_N; s_N) d\boldsymbol{r}_1 d\boldsymbol{r}_1 ... d\boldsymbol{r}_1 ds_1 ds_2 ... ds_N. \end{aligned} \tag{4.8}$$

With such a definition, eq. (4.2) can be expressed for the average field as [19]

$$< u(\boldsymbol{r}) > = u^0(\boldsymbol{r}) + \sum_j \int_V \int P(\boldsymbol{r}_j; s_j) T(\boldsymbol{r}_j, s_j) < u^j(\boldsymbol{r}) >_j E(\boldsymbol{r}, \boldsymbol{r}_j) d\boldsymbol{r}_j ds_j, \tag{4.9}$$

where $< u(\boldsymbol{r}) >$ is the coherent field propagating in the medium and $< u^j(\boldsymbol{r}) >_j$ is the effective field acting on the jth scatterer. The effective field is the average over all scatterers excluding the jth scatterer. Foldy [19] approximately considered the effective field to be equal to the coherent field ($< u^j(\boldsymbol{r}) >_j = < u(\boldsymbol{r}) >$). Twersky [35] showed that this approximation is valid for the scattering events in which a scatterer contributes in the scattering process only once. This is shown in fig. 4.1 where Foldy approach is valid for the scattering events in fig. 4.1(a) [38]. The scattering events of fig. 4.1(b) are effective when the scatterers are close to each other and back scattering is considerable. For such cases Lax [33] considered correlation between pairs of scatterers and defined a constant c so that $< u^j(\boldsymbol{r}) >_j = c < u(\boldsymbol{r}) >$ to distinguish between the effective field and the coherent field. Waterman and Truell [36] also derived a more complex relation for the effective field by considering back scattering of the scatterers.

Here only the Foldy approximation is considered. Hence, the eq. (4.9) can be written as

$$< u(\boldsymbol{r}) > = u^0(\boldsymbol{r}) + < u(\boldsymbol{r}) > \int_V \int n(\boldsymbol{r}_j; s_j) T(\boldsymbol{r}_j, s_j) E(\boldsymbol{r}, \boldsymbol{r}_j) d\boldsymbol{r}_j ds_j. \tag{4.10}$$

For many problems the state of a scatterer is not related to its location and $n(\boldsymbol{r}_j; s_j) = n(\boldsymbol{r}_j)\alpha(s_j)$. Furthermore for a homogeneous distribution of scatterers $n_r(\boldsymbol{r}_j) = n = N/V$.

Applying the operator $\nabla^2 + k^2$ to eq. (4.10) and taking the integration leads to

$$(\nabla^2 + k^2) < u(\boldsymbol{r}) > = -4\pi n < u(\boldsymbol{r}) > \bar{T}(\boldsymbol{r}), \tag{4.11}$$

where

$$\bar{T}(\boldsymbol{r}) = \int \alpha(s) T(\boldsymbol{r}, s) ds. \tag{4.12}$$

For a macroscopically homogeneous medium $\bar{T}(\boldsymbol{r})$ is constant and can be considered as the average forward scattering amplitude of the scatterers ($\bar{f}$) [33, 39]. Therefore eq. (4.11) becomes

$$\begin{aligned} &(\nabla^2 + K^2) < u(\boldsymbol{r}) >= 0, \\ &K^2 = k^2 + 4\pi n \bar{f}(K), \end{aligned} \tag{4.13}$$

where K is the effective wave number of the coherent field in the medium and $\bar{f}(K)$ indicates that the effective field acting on the scatterers is considered to be equal to the coherent field as considered by Foldy. A simpler approximation is to consider $u^0(\boldsymbol{r})$ as the field acting on all scatterers ($\bar{f}(k)$). This is then referred to as simple Foldy theory [37].

Generally, the parameter $\bar{f}(K)$ is complex even for a lossless scatterer. So the average effective field $< u >$ attenuates as it propagates through the medium. This is of course due to scattering and is related to the scattering amplitude. Clearly in this approximation it is assumed first that the effective field acting on each scatterer is the same for every scatterer and also that the scattered wave propagates in the k medium as if there is no other scatterer. These assumptions together with the far field approximation of $E(\boldsymbol{r}, \boldsymbol{r}_j)$ are more reliable for a dilute distribution of scatterers (small values of N). Overall, the validity of these approximations are best to be justified by actual physical behaviour of the medium and the experimental results. Such studies have shown that there are cases that even the simpler approximations like Foldy and Lax theory show better estimation of the effective field properties than more refined theories [40]. For a comprehensive comparison among different approximation regarding the effective field acting on scatterers one can refer to [37].

4.2 Continuous random media

In the macroscopic approach the Helmholtz equation (eq. (4.1)) is substituted by an equation with a random coefficient [32]

$$(\nabla^2 + k^2 + \epsilon(r) k^2) u = 0, \tag{4.14}$$

where k is the wave number of the mean homogeneous field and $\epsilon(r)$ is the centered random fluctuation with respect to k. Considering the radiation condition and the outward radiating Green function of the homogeneous medium

$$G^{(0)}(\boldsymbol{r},\boldsymbol{r'}) = \frac{e^{ik|\boldsymbol{r}-\boldsymbol{r'}|}}{4\pi|\boldsymbol{r}-\boldsymbol{r'}|}, \tag{4.15}$$

the following random integral equation can be used instead of the wave equation

$$G(\boldsymbol{r},\boldsymbol{r}') = G^{(0)}(\boldsymbol{r},\boldsymbol{r}_1) - k^2 \int_{V_t} G^{(0)}(\boldsymbol{r},\boldsymbol{r}')\epsilon(\boldsymbol{r}_1)G(\boldsymbol{r}_1,\boldsymbol{r}')d\boldsymbol{r}_1, \tag{4.16}$$

where $G(\boldsymbol{r},\boldsymbol{r}')$ is the Green's function of the inhomogeneous medium. This equation is solved by formal iteration which leads to the following perturbation series

$$\begin{aligned} G(\boldsymbol{r},\boldsymbol{r}') = G^{(0)}(\boldsymbol{r},\boldsymbol{r}_1) - k^2 \int_{V_t} G^{(0)}(\boldsymbol{r},\boldsymbol{r}')\epsilon(\boldsymbol{r}_1)G^{(0)}(\boldsymbol{r}_1,\boldsymbol{r}')d\boldsymbol{r}_1 \\ + k^4 \int_{V_t}\int_{V_t} G^{(0)}(\boldsymbol{r},\boldsymbol{r}_2)\epsilon(\boldsymbol{r}_2)G^{(0)}(\boldsymbol{r}_2,\boldsymbol{r}_1)\epsilon(\boldsymbol{r}_1)G^{(0)}(\boldsymbol{r}_1,\boldsymbol{r}')d\boldsymbol{r}_1 d\boldsymbol{r}_2 + ... \end{aligned} \tag{4.17}$$

The second integral in this equation corresponds to a wave which propagates freely from $\boldsymbol{r}'$ to $\boldsymbol{r}_1$, is scattered by the random inhomogeneity at $\boldsymbol{r}_1$, propagates freely from $\boldsymbol{r}_1$ to $\boldsymbol{r}_2$, is scattered at $\boldsymbol{r}_2$ and propagates to $\boldsymbol{r}$; similarly for higher orders of the perturbation series. Therefore the equation has a physical interpretation in terms of multiple scattering. Solving the series of integral equations (4.17) for the mean Green function leads to the Dyson integral equation [32]

$$\begin{aligned} < G(\boldsymbol{r},\boldsymbol{r}') > = G^{(0)}(\boldsymbol{r},\boldsymbol{r'}) - k^2 \int_{V_t} G^{(0)}(\boldsymbol{r},\boldsymbol{r}')G^{(0)}(\boldsymbol{r}_1,\boldsymbol{r}') < \epsilon(\boldsymbol{r}_1) > d\boldsymbol{r}_1 \\ + k^4 \int_{V_t}\int_{V_t} G^{(0)}(\boldsymbol{r},\boldsymbol{r}_2)G^{(0)}(\boldsymbol{r}_2,\boldsymbol{r}_1)G^{(0)}(\boldsymbol{r}_1,\boldsymbol{r}') < \epsilon(\boldsymbol{r}_1)\epsilon(\boldsymbol{r}_2) > d\boldsymbol{r}_1 d\boldsymbol{r}_2 + ... \end{aligned} \tag{4.18}$$

Normally the random fluctuations are defined to have zero mean, meaning $<\epsilon(\boldsymbol{r}_1)>= 0$ and the first integral in the perturbation series is zero and the others depend on higher orders moments of $\epsilon(\boldsymbol{r})$ as $<\epsilon(\boldsymbol{r}_1)\epsilon(\boldsymbol{r}_2)...\epsilon(\boldsymbol{r}_n)>$. Taking a spatial Fourier transform of the Dyson integral equation leads to the following dispersion equation for the effective wave number of the inhomogeneous medium [32]

$$K^2 = k^2 - M(\boldsymbol{K}), \tag{4.19}$$

where $M(\boldsymbol{K})$ is the Fourier transform of the mass operator related to the sum of all integral terms in the perturbation series which can also be expressed using the diagrammatic method [32]. A common approximation introduced by Bourret [41] is to only consider the first term of the mass operator, which means that only the covariance of the random fluctuations ($<\epsilon(\boldsymbol{r}_1)\epsilon(\boldsymbol{r}_2)>$) is considered. This approximation is consistent with the first order smoothing approximation in the method of smoothing as followed by Keller for random differential equations [42]. The covariance of random fluctuations is then calculated by a two point correlation function showing the probability of two points lying in the same inhomogeneity. The details of this approach and its analogy with other methods like smoothing and multiple scattering theory is comprehensively discussed by Frisch [32]. It is worth mentioning that the Dyson integral equation (4.18) and the integral equation for multiple scattering theory (eq. (4.10)) exhibit a clear analogy with each other. The fundamental difference lies in the definition of the scattering characteristics. In multiple scattering theory, it is defined by the scattering amplitude of individual scatterers, while in the Dyson equation, it is defined by the covariance of the elastic properties fluctuation between two arbitrary points in the random medium.

Most of the early studies on wave propagation in an inhomogeneous medium are considering a medium which is locally isotropic. For the case that inhomogeneities are anisotropic, e.g. polycrystalline materials, only the macroscopic approach has been applied, thus defining the anisotropy by fluctuations with respect to a reference isotropic homogeneous medium. The objective of the present study is to examine the influence of incorporating the scattering characteristics of an anisotropic scatterer in the approximation of the mean field in an inhomogeneous material. This investigation is carried out within the framework of the simple and self consistent Foldy approach. This is particularly investigated for single phased polycrystalline materials with randomly oriented grains of different anisotropy symmetry. The application of the microscopic and macroscopic approach for the elastic waves propagating in polycrystalline materials is discussed in the next section.

4.3 Polycrystalline materials

Polycrystalline materials are solids that consist of many small crystals which are usually called grains. The grains are usually anisotropic, have often random orientations and are separated by grain boundaries. When the anisotropic grains are oriented randomly, the macroscopic behaviour of the medium is isotropic. Propagation of a wave through polycrystalline materials can be considered as a special case of a random inhomogeneous medium with local anisotropy. The interest of the current study is mainly to investigate the overall average response of the polycrystalline material, rather than the local effects of individual grains. Therefore, the basic idea is to model the original, inhomogeneous polycrystal as a statistically homogeneous and isotropic medium, which should have the same overall average response.

Most recent studies model polycrystalline materials as a continuous medium with an isotropic reference medium and anisotropic random fluctuations. The method of solution then follows the concepts discussed in section 4.2. However, as the anisotropy of the grains increases, the fluctuations with respect to the reference medium also increase, causing this method to lose its accuracy. In the present research another approach based on the theory of Foldy [19] is used to calculate attenuation and effective phase velocity of the waves in polycrystalline materials. This theory was developed for waves propagating in an acoustic medium with a distribution of point scatterers, but has been generalized to the elastic case with bounded obstacles [43, 44]. In this section first a review of the former approach is presented, then application of the Foldy theory is discussed for polycrystalline materials.

Stochastic model for polycrystalline materials

A classical approach to study polycrystalline materials is to replace the micro-inhomogeneous elastic polycrystal with a continuous random medium described by a local elastic stiffness tensor $C_{ijkl}(\boldsymbol{r}) = c_{ijkl} + \delta_{ijkl}(\boldsymbol{r})$ with mean isotropic stiffness c_{ijkl} and random fluctuations $\delta_{ijkl}(\boldsymbol{r})$. The fluctuations with respect to the mean elastic tensor $\delta_{ijkl}(\boldsymbol{r})$ are considered to be small and the mean elastic medium with tensor c_{ijkl} is called the reference medium and for a single phase polycrystalline is normally considered to be the Voigt average of the grain properties [23]. The elastodynamic differential equations with random coefficients are then solved using the diagrammatic method and the Bourret approximation of the Dyson integral equation [40] or the Keller first order smoothing approximation [15], which are shown to be equivalent to each other [23]. Following the diagrammatic method as described in section 4.2, the elastodynamic equation can be reduced to the Dyson integral equation for the mean Green function as [23]

$$< G_{k\alpha}(\boldsymbol{r},\boldsymbol{r'}) > = G^{(0)}_{k\alpha}(\boldsymbol{r},\boldsymbol{r'}) + \int_{V_t}\int_{V_t} G^{(0)}_{k\beta}(\boldsymbol{r},\boldsymbol{r}_2) M_{\beta j}(\boldsymbol{r}_2,\boldsymbol{r}_1) < G_{j\alpha}(\boldsymbol{r_1},\boldsymbol{r'}) > d\boldsymbol{r}_1 d\boldsymbol{r}_2, \tag{4.20}$$

where $G_{k\alpha}(\boldsymbol{r},\boldsymbol{r'})$ is the k direction displacement response at $\boldsymbol{r}$ due to α direction impulse at $\boldsymbol{r'}$, $G^{(0)}_{k\alpha}(\boldsymbol{r},\boldsymbol{r'})$ is the same for the reference isotropic medium and $M_{\beta j}$ is the mass operator for the j direction impulse and β direction response waves. The mass operator is a function of the random fluctuation covariance $< \delta_{ijkl}(\boldsymbol{r}), \delta_{\alpha\beta\gamma\zeta}(\boldsymbol{r}) >$. A vital element of the theory is the incorporation of the covariance of the elastic tensor in the mass operator using a statistical two-point correlation (TPC) between $\boldsymbol{r}$ and $\boldsymbol{r'}$. For a statistically homogeneous polycrystal, the covariance can be factored into elastic and spatial parts by $< \delta_{ijkl}(\boldsymbol{r}), \delta_{\alpha\beta\gamma\zeta}(\boldsymbol{r}) >=< \delta_{ijkl}, \delta_{\alpha\beta\gamma\zeta} > w(\boldsymbol{r}-\boldsymbol{r'})$. The elastic part is solely determined by the elastic constants of the polycrystal. The spatial part $w(\boldsymbol{r}-\boldsymbol{r'})$ is the well-known spatial TPC function describing the probability of two points being in the same grain. The spatial TPC function is related to the size and shape of the grains. The TPC function can also be defined in a way to capture various volume distribution of grains or even non equiaxed grains [25, 45, 46, 47]. This model is generally called the second order approximation (SOA) since it is accurate when second-order degrees of inhomogeneity is small. Using the Fourier transform in the Dyson equation leads to the following dispersion equation for the perturbed wavenumber K [23]

$$K_i^2 = k_i^2 - \frac{m_i(\mathbf{K})}{V_{0i}}. \tag{4.21}$$

Here K is the effective wave number of the polycrystalline medium, $\mathbf{K} = K\mathbf{p}$ is the vector wave number with $\mathbf{p}$ being the wave propagation direction, and V_{0i} and $m_i = \sum_{j=P,S} m_{ij}$ are the Voigt phase velocity and mass operator respectively, with $i = S$ for transverse waves and $i = P$ for longitudinal waves. The mass operator includes different scattering events and are generally in form of Cauchy integrals which can be studied numerically for different classes of anisotropy [17, 25, 48, 49]. Using the far field approximation, the mass operator is approximated with an explicit expression without involving calculation of Cauchy integrals [50]. These methods normally do not lead to a closed form solution for the perturbed wave number K unless invoking more assumptions like the Born approximation, the Rayleigh asymptote (valid for low frequencies) or the stochastic asymptote (valid for high frequencies).

Foldy theory for polycrystalline materials

Foldy theory, which is described in section 4.1 for scalar waves and point scatterers, is developed for elastic waves and bounded obstacles as [43, 44]

$$K_i^2 = k_i^2 + 4\pi n \bar{f}_i, \tag{4.22}$$

where the index i can be P or S for longitudinal and transverse waves, K_i and k_i are the wave numbers of the effective medium and the medium surrounding the scatterers, respectively. For a case with all scatterers having same volume V_s and relative density d, $n = d/V_s$. The average forward scattering amplitude $\bar{f}_i$ can be related to the transition matrix defined in chapter 3 as [51]

$$\begin{aligned} \bar{f}_p &= -\frac{i}{k_p} \sum_{\sigma ml} T_{3\sigma ml, 3\sigma ml}, \\ \bar{f}_s &= -\frac{i}{2k_s} \sum_{\substack{\tau\sigma ml \\ \tau=1,2}} T_{\tau\sigma ml, \tau\sigma ml}. \end{aligned} \tag{4.23}$$

The average dynamic response of the medium including attenuation and phase velocity can be described by the real and imaginary parts of the effective wave number

$$\begin{aligned} \frac{\alpha_i}{k_i} &= \operatorname{Im} \frac{K_i}{k_i}, \\ \frac{C_i}{c_i} &= \operatorname{Re} \frac{k_i}{K_i}. \end{aligned} \tag{4.24}$$

In polycrystalline materials, the grains fill the medium, and the surrounding medium of each grain is not a known homogeneous medium, as required by the Foldy theory. Thus, single phase polycrystalline materials first need to be homogenized through some form of averaging over the elastic properties of the grains. This assumption is generally referred to as the effective medium approach and differs from the effective field approach as described in section 4.1. A comprehensive overview of both the effective field and effective medium approaches is available in the literature [52].

In this context, a homogeneous medium is initially defined for the polycrystalline material, followed by the utilization of the simple Foldy theory to evaluate attenuation and phase velocity within the medium. In summary, the following assumptions for the medium and the propagating wave are considered.

1. Each grain is considered to be isolated from all other grains, and they all experience the same incident wave.

2. The simple Foldy theory is followed in which the forward scattering amplitude is evaluated for an exciting field similar to a field propagating in the homogenized reference medium without any grains. This implies that each grain contributes to scattering only once, and the scattered field of one grain does not affect the fields acting on other grains.

3. The scattered wave is studied in the far field of the grains.

4. As the grains fill the medium in the polycrystalline materials, their distribution density is $d = 1$. Therefore the total number density of the inclusions is calculated as $n = 1/V_s$, V_s being the average volume of the grains.

5. The size of the scatterers is much smaller than the wavelength of the incident wave.

The best way to validate these assumptions is to compare the results with experimental data. However, the approach in this study, instead, compares with numerical FEM results, which have demonstrated reasonable correspondence with empirical investigations [22]. This comparison is studied in Papers B, C, and D for polycrystalline materials with transversely isotropic, cubic, and orthotropic grain properties, respectively. In these papers, the properties of the homogenized medium are considered to be the Voigt average of the grain properties. Furthermore, in Papers C and D, a self consistent effective medium approach is also adopted, where the approximated homogenized medium k is equated to the effective homogenized medium K in the static limit. With such an assumption, the effective field acting on the grains is the coherent field propagating in the inhomogeneous medium which fulfills the assumption of Foldy theory. In Paper E, the effects of grain size are investigated by incorporating a grain size distribution instead of a single grain size V_s. Additionally, in Paper E, the application of the present approach is extended to encompass multiphase polycrystalline materials.

5 Summary of Appended Papers

5.1 Paper A

In this paper, a single anisotropic spherical obstacle contained in a three-dimensional, homogeneous, isotropic and infinite elastic medium is considered. For this canonical problem a transversely isotropic sphere is considered in which the axis of material symmetry is perpendicular to the xy plane. A spherical coordinate system (r, θ, φ) is set at the center of the sphere and an incident plane wave propagates in the z direction. Such a restriction on the incident wave makes the problem rotationally symmetric and consequently the displacement and stress fields are independent of the azimuthal angle φ. Based on the polarization of the incident wave the problem can be decomposed into two independent problems, one relating to motion in the φ direction (torsional waves, also known as SH waves) and the other relating to motion in the $r\theta$ plane (P-SV waves). Only the SH waves which is a scalar case is considered in Paper A.

To solve the problem, the displacement field in the isotropic medium outside the sphere is constructed as a superposition of incident and scattered waves, which are expanded in spherical vector wave functions. In the anisotropic sphere first the elastodynamic equations are transformed into spherical coordinates and then the displacement field is expanded in associated Legendre functions in θ and powers in r. Substituting the expansion into the equation of motion inside the sphere leads to recursion relations for the expansion coefficients that couple different polar orders (in contrast to an isotropic sphere where there is no such coupling). Using the boundary conditions on the surface of the sphere results in a system of equations for all the expansion coefficients for the fields outside and inside the sphere. As a result, the transition ($\mathbf{T}$) matrix elements are calculated and given explicitly for low frequencies. Some numerical examples of scattered far fields are also presented.

5.2 Paper B

Paper B continues the work presented in Paper A. In this paper, the same problem as in Paper A is addressed; however, this time, no restrictions are imposed on the incident wave. This means that the incident wave can take the form of a plane wave of any type in any direction. Consequently, the axisymmetric assumption made in Paper A becomes invalid, and all fields now depend on all spherical coordinates.

The general methodology employed in this paper closely resembles that of Paper A. Here again the elastodynamic equations inside the sphere are transformed to spherical coordinates and the displacement field is expanded in the vector spherical harmonics in the angular coordinates and powers in the radial coordinate. Then recurrence relations among the expansion coefficients can be found using the governing equations inside the sphere. In the surrounding medium the displacement and traction fields are expanded in terms of the spherical vector wave functions. All the remaining expansion coefficients for the fields outside and inside the sphere are found using the boundary conditions on the surface of the sphere. As a result, the transition ($\mathbf{T}$) matrix elements are calculated and given explicitly for low frequencies.

In Paper B, this $\mathbf{T}$ matrix is utilized to investigate wave propagation within polycrystalline materials characterized by transversely isotropic grains. Foldy theory is employed to derive an explicit expression for the effective complex wave number of such materials, particularly focusing on low frequencies. The paper considers the macroscopic homogenized medium to be the Voigt average of the grain properties.

Subsequently, the attenuation coefficients and phase velocities of waves within the material are directly deduced from the effective wave number. These quantities are numerically compared with previously published results and with recent FEM results. The comparison with FEM for low frequencies shows a good agreement regardless of the degree of anisotropy while the validity of other published methods is restricted to weakly anisotropic materials.

5.3 Paper C

In Paper C, the same problem addressed in Paper B is considered, with the distinction that the anisotropic sphere exhibits cubic anisotropy. The approach to solving the problem remains identical with the methodology outlined in Paper B. The adoption of cubic anisotropy brings about an advantage in mathematical computations, as it involves only three independent elastic coefficients. In contrast, transversely isotropic materials are characterized by five elastic constants. However, it is noteworthy that transversely isotropic materials exhibit a rotationally symmetric behavior, leading to the absence of coupling between different orders of incident and scattered waves in the φ direction. On the other hand, this symmetry is not present in cubic materials. Consequently, coupling arises among orders of m and $m \pm 4$ of the incident and scattered waves in the azimuthal direction, as detailed in the paper. In the low-frequency limit, where only orders of $m = 0, 1$, and 2 are relevant, such coupling becomes negligible, and the $\mathbf{T}$ matrix elements are derived in a similar manner as described in Paper B.

Furthermore, similar to Paper B, this paper investigates single phase equiaxed polycrystalline materials. The focus here is on polycrystalline materials with grains exhibiting cubic anisotropy. An advancement in this study is related to the treatment of macroscopic homogenized properties. In addition to the conventional Voigt average, which is commonly employed in this context, a self consistent approach is adopted in Paper C. It is assumed that the macroscopic homogenized medium has the same properties as the effective medium in the low frequency limit. It is demonstrated that this is equivalent to defining the surrounding medium of the sphere in such a manner that, in the low frequency limit, the average far field scattering amplitude possesses only an imaginary component. Consequently, this approach leads to a set of polynomial equations that govern the elastic constants of the effective homogenized medium in the low frequency limit. When comparing the results with FE evaluations, it indicates that this method yields a better agreement than the Voigt average.

5.4 Paper D

In Paper D, the previous studies are extended to encompass a more general scenario, involving the orthorhombic symmetry of the spherical obstacles. A material exhibiting such symmetry can be characterized by nine distinct elastic coefficients, which significantly elevate the complexity of the governing equations. Expressing the constituent relation of such a medium in spherical coordinates reveals that coupling exists among m, $m \pm 2$, and $m \pm 4$ orders of the incident and scattered waves in the azimuthal direction. Consequently, it becomes evident that in the low frequency limit, the orders $m = 0$ and $m = 2$ become coupled, resulting in a larger system of equations that need to be simultaneously solved.

The resulting **T** matrix elements exhibit interesting dependence on the elastic coefficients of the spherical obstacles. As discussed in the paper, for dipole elements ($l = 1$), the T matrix only depends on the density of the sphere (ρ_1). This is well understood as it corresponds to rigid body translation. For monopole elements ($l = 0$), which are coupled with even quadrupole elements ($l = 2$ with $\sigma = e$), the T matrix elements only depend on the elasticity of the sphere and its surrounding medium but not on the density or shear moduli (C_{44}, C_{55}, and C_{66}). For odd quadrupole elements ($l = 2$ with $\sigma = o$), the T matrix elements only depend on the shear moduli of the sphere.

These **T** matrix elements are subsequently employed to investigate 50 distinct single phase polycrystalline materials with various type of anisotropy. The established system of polynomial equations, employed for determining the effective medium properties in the static limit, is demonstrated to yield results consistent with the conventional self consistent averaging of an anisotropic crystal. Furthermore, the FE evaluation of phase velocity and attenuation within these materials highlights a good agreement with the present method. This agreement is particularly evident when the macroscopic homogenized medium is regarded as equivalent to the effective medium.

5.5 Paper E

Paper E aims to investigate attenuation and phase velocity within polycrystalline materials, incorporating diverse statistical information concerning the properties of the grains. By adopting the Foldy methodology, the statistical details are encompassed in the ensemble average of the forward scattering amplitude of the grains. Specifically, two scenarios are considered for the cases where the average is calculated across grains with varying mechanical properties or when this average encompasses a distribution of grain sizes.

The examination of the grain size distribution reveals that the low frequency phase velocity remains unaffected by the grain size distribution. Conversely, the attenuation within polycrystalline materials displays a dependency on the third moment of the grain size distribution. When comparing the method presented here with previously analytical published results, a good correspondence is observed within the low frequency limit for weakly anisotropic crystals. For materials exhibiting strong anisotropy, however, significant differences occur as expected. These results confirm that the influence of the grain size distribution remains independent of the degree of anisotropy.

Furthermore, an examination of the variation in the mechanical properties of the grains is conducted for duplex polycrystalline materials. Two cases are studied: one with a significant difference and another with a minor difference in the mechanical properties between the two phases. The evaluation is conducted for attenuation and phase velocity in the low frequency limit for different volume concentrations of the distinct phases. A comparison with published findings demonstrates a reasonable agreement.

6 Concluding Remarks and Future Work

This thesis demonstrates an analytical approach to study scattering by an anisotropic sphere. An advantage of analytical approaches is the valuable insights of the various aspects of the problem. Particularly noteworthy is the dependence of stresses in spherical coordinates on the trigonometric functions of the angular coordinates. The thesis highlights how such dependence results in coupling between different orders of the incident wave, a phenomenon absent in isotropic cases. By employing a systematic series expansion involving suitable orthogonal functions in the angular directions and power series in the radial direction, recursion relations are established among the expansion coefficients. The boundary conditions on the sphere are then used to determine the elements of the transition matrix (**T**).

Another insight comes from the explicit expressions of the **T** matrix elements for low frequencies. It can clearly be observed that for low frequencies it is the P-SV waves that play a dominant role and the SH waves are of limited interest. To be more specific, the leading order **T** matrix elements of the SH waves behave as $(ka)^5$ while for the P-SV waves they behave as $(ka)^3$. Furthermore, such explicit expressions clearly demonstrate how different **T** matrix elements depend on the stiffness constants and density of the sphere and the surrounding medium.

One important application of these **T** matrices is to derive the forward scattering amplitude of an anisotropic obstacle. With the analytical expression of this parameter and using Foldy theory explicit expressions for attenuation coefficients and effective phase velocities in a polycrystalline materials with various anisotropy of the grains are derived. Although these expressions are limited to low frequencies, they have no restriction on the polycrystalline degree of anisotropy in contrast to other published analytical approaches.

An inherent advantage of possessing explicit expressions for the forward scattering amplitude is the capability to seamlessly incorporate an inhomogeneous medium, where the scatterers may exhibit a range of distinct forward scattering amplitudes. This feature proves particularly valuable, as it allows for the evaluation of the average forward scattering amplitude in the presence of a specific distribution of scatterers. While this idea has been extensively explored in the existing literature, with a primary focus on isotropic scatterers, the findings of this study contribute to the extension of these methodologies to encompass scenarios involving anisotropic scatterers. This is specifically followed for a grain size distribution of the scatterers and a medium with multiple type of scatterers in polycrystalline materials. There is no particular problem in extending the study for other scenarios such as volume concentration of the scatterers in particulate composites. Generally, extension of the forward scattering amplitude for an isotropic obstacle to an anisotropic one, marks a step forward in broadening the applicability of the existing approaches for analysing dynamic response of inhomogeneous materials to a wider array of real world situations.

A possible extension of the current work is to explore somewhat higher frequencies. This requires deriving explicit expressions for the traction on the surface of the sphere for any desired expansion of the displacement field within the sphere. Additionally, it is necessary to have the recursion relation among the expansion coefficients analytically as well. Although this was followed in the simple case of Paper A, for the general case, it remained unsolved due to the complexity of the mathematical relations. Alternatively, the $\mathbf{T}$ matrix and forward scattering amplitude can be computed numerically. When applying them to inhomogeneous media, the limitations of the Foldy approach used so far may become important. Therefore, other multiple scattering theories, briefly mentioned here, may offer better accuracy at higher frequencies and can be considered.

The proposed approach can be extended to address a more intricate scenario, involving an isotropic elastic interface in conjunction with an anisotropic sphere positioned within an isotropic matrix featuring properties that differ from those of the interface. This is followed in the literature for an isotropic sphere [53] and an extension for an anisotropic sphere would be valuable. This may have particular interest in polycrystalline materials when there is an interface with distinct material properties around the grains. Furthermore, an effective medium approach to evaluate particulate composite dynamic response is to study scattering by a single sphere when it is located in a matrix with effective properties of the constituent while in the vicinity of the sphere there is a layer with mechanical properties of the actual hosting medium of the composite [52].

Another interesting research problem involves examining the scattering behavior of a sphere with electro-magneto-elastic properties, situated within an elastic and isotropic medium. Since electro-magneto-elastic mediums are typically anisotropic, the proposed approach remains applicable, though with additional complexities related to the propagation of electric and magnetic waves and their coupling with elastic waves in the sphere.

References

[1] C. Zhang and D. Gross. *On wave propagation in elastic solids with cracks.* Computational Mechanics Publications, Southampton, 1998.

[2] A. T. de Hoop. *Handbook of radiation and scattering of waves: acoustic waves in fluids, elastic waves in solids, electromagnetic waves.* Academic Press, San Diego, 1995.

[3] V. V. Varadan, A. Lakhtakia, and V. K. Varadan. *Field representations and introduction to scattering.* North-Holland, Amsterdam, 1991.

[4] C. Wan and H. Li. Analytical Method and Semianalytical Method for Analysis of Scattering by Anisotropic Sphere: A Review. *International Journal of Antennas and Propagation* **2012** (2012), 782320.
[5] A. Doicu. Null-field method to electromagnetic scattering from uniaxial anisotropic particles. *Optics communications* **218** (2003), 11–17.
[6] J. J. Wang et al. Electromagnetic scattering from gyroelectric anisotropic particle by the T-matrix method. *Journal of Quantitative Spectroscopy and Radiative Transfer* **135** (2014), 20–29.
[7] P. A. Martin and J. R. Berger. Waves in wood: free vibrations of a wooden pole. *Journal of the Mechanics and Physics of Solids* **49** (2001), 1155–1178.
[8] S. M. Hasheminejad and M. Maleki. Acoustic resonance scattering from a submerged anisotropic sphere. *Acoustical Physics* **54** (2008), 168–179.
[9] A. N. Norris and A. L. Shuvalov. Elastodynamics of radially inhomogeneous spherically anisotropic elastic materials in the Stroh formalism. *Proceedings of the Royal Society A: Mathematical, Physical and Engineering Sciences* **468** (2012), 467–484.
[10] M. D. Guild, A. Alù, and M. R. Haberman. Cloaking of an acoustic sensor using scattering cancellation. *Applied Physics Letters* **105** (2014), 023510.
[11] M. Y. Chung. Stress Amplification/Shielding Phenomena of Spherically Anisotropic and Radially Inhomogeneous Linear Elastic Hollow Spheres. *The Quarterly Journal of Mechanics and Applied Mathematics* **72** (2019), 535–544.
[12] A. Boström. Scattering by an anisotropic circle. *Wave Motion* **57** (2015), 239–244.
[13] A. Boström. Scattering of in-plane elastic waves by an anisotropic circle. *The Quarterly Journal of Mechanics and Applied Mathematics* **71** (2018), 139–155.
[14] E. R. Pike and P. C. Sabatier. *Scattering: scattering and inverse scattering in pure and applied science.* Academic Press, New York, 2001.
[15] F. E. Stanke and G. S. Kino. A unified theory for elastic wave propagation in polycrystalline materials. *The Journal of the Acoustical Society of America* **75**.3 (1984), 665–681.
[16] R. B. Thompson et al. Scattering of elastic waves in simple and complex polycrystals. *Wave Motion* **45**.5 (2008), 655–674.
[17] L. Yang, O. I. Lobkis, and S. I. Rokhlin. Explicit model for ultrasonic attenuation in equiaxial hexagonal polycrystalline materials. *Ultrasonics* **51**.3 (2011), 303–309.
[18] J. Li and S. I. Rokhlin. Elastic wave scattering in random anisotropic solids. *International Journal of Solids and Structures* **78** (2016), 110–124.
[19] L. L. Foldy. The multiple scattering of waves. I. General theory of isotropic scattering by randomly distributed scatterers. *Physical Review* **67**.3-4 (1945), 107.
[20] A. Boström and A. Ruda. Ultrasonic attenuation in polycrystalline materials in 2D. *Journal of Nondestructive Evaluation* **38**.2 (2019), 1–6.
[21] A. Van Pamel et al. Finite element modelling of elastic wave scattering within a polycrystalline material in two and three dimensions. *The Journal of the Acoustical Society of America* **138**.4 (2015), 2326–2336.
[22] A. Van Pamel et al. Finite-element modelling of elastic wave propagation and scattering within heterogeneous media. *Proceedings of the Royal Society A: Mathematical, Physical and Engineering Sciences* **473**.2197 (2017), 2016–0738.

[23] A. Van Pamel et al. Numerical and analytic modelling of elastodynamic scattering within polycrystalline materials. *The Journal of the Acoustical Society of America* **143**.4 (2018), 2394–2408.
[24] M. Ryzy et al. Influence of grain morphology on ultrasonic wave attenuation in polycrystalline media with statistically equiaxed grains. *The Journal of the Acoustical Society of America* **143**.1 (2018), 219–229.
[25] G. Sha et al. Attenuation and velocity of elastic waves in polycrystals with generally anisotropic grains: Analytic and numerical modeling. *The Journal of the Acoustical Society of America* **147**.4 (2020), 2442–2465.
[26] M. Huang et al. Maximizing the accuracy of finite element simulation of elastic wave propagation in polycrystals. *The Journal of the Acoustical Society of America* **148**.4 (2020), 1890–1910.
[27] M. Huang et al. Finite-element and semi-analytical study of elastic wave propagation in strongly scattering polycrystals. *Proceedings of the Royal Society A: Mathematical, Physical and Engineering Sciences* **478**.2258 (2022), 20210850.
[28] M. Huang, S. I. Rokhlin, and M. J. S. Lowe. Appraising scattering theories for polycrystals of any symmetry using finite elements. *Philosophical Transactions of the Royal Society A: Mathematical, Physical and Engineering Sciences* **380**.2231 (2022), 20210382.
[29] J. Achenbach. *Wave propagation in elastic solids.* North-Holland, London, 1973.
[30] A. C. Eringen and E. S. Suhubi. *Elastodynamics, vol. II: linear theory.* Academic Press, New York, 1975.
[31] P. A. Martin. *Multiple scattering: interaction of time-harmonic waves with N obstacles.* 107. Cambridge University Press, New York, 2006.
[32] U. Frisch. "Wave propagation in random media." *Probabilistic Methods in Applied Mathematics.* Ed. by A. T. Bharucha-Reid. Vol. 1. Academic Press, New York, 1968.
[33] M. Lax. Multiple scattering of waves. *Reviews of Modern Physics* **23**.4 (1951), 287.
[34] H. S. Snyder and W. T. Scott. Multiple scattering of fast charged particles. *Physical Review* **76**.2 (1949), 220–225.
[35] V. Twersky. "On propagation in random media of discrete scatterers". *Proceedings of Symposia in Applied Mathematics.* Ed. by R. Bellman. Vol. 16. American Mathematical Society, New York, 1964, pp. 84–116.
[36] P. C. Waterman and R. Truell. Multiple scattering of waves. *Journal of mathematical physics* **2**.4 (1961), 512–537.
[37] L. W. Anson and R. C. Chivers. Ultrasonic velocity in suspensions of solids in solids—A comparison of theory and experiment. *Journal of Physics D: Applied Physics* **26**.10 (1993), 1566.
[38] A. Ishimaru. *Wave propagation and scattering in random media, Vol 2.* Academic press, New York, 1978.
[39] J. Mittleman. *Ultrasonic scattering from decorated grain boundaries.* Iowa State University, 1995.
[40] R. L. Weaver. Diffusivity of ultrasound in polycrystals. *Journal of the Mechanics and Physics of Solids* **38**.1 (1990), 55–86.
[41] R. C. Bourret. Stochastically perturbed fields, with applications to wave propagation in random media. *Il Nuovo Cimento (1955-1965)* **26** (1962), 1–31.

[42] J. B. Keller. “Stochastic equations and wave propagation in random media”. *Proceedings of Symposia in Applied Mathematics*. Ed. by R. Bellman. Vol. 16. American Mathematical Society, New York, 1964, pp. 145–179.
[43] S. K. Datta et al. Phase velocity and attenuation of plane elastic waves in a particle-reinforced composite medium. *Wave Motion* **10**.2 (1988), 171–182.
[44] J. E. Gubernatis and E. Domany. Effects of microstructure on the speed and attenuation of elastic waves in porous materials. *Wave Motion* **6**.6 (1984), 579–589.
[45] L. Yang, O. I. Lobkis, and S. I. Rokhlin. Shape effect of elongated grains on ultrasonic attenuation in polycrystalline materials. *Ultrasonics* **51**.6 (2011), 697–708.
[46] O. I. Lobkis et al. Ultrasonic backscattering in polycrystals with elongated single phase and duplex microstructures. *Ultrasonics* **52**.6 (2012), 694–705.
[47] J. Li, L. Yang, and S. I. Rokhlin. Effect of texture and grain shape on ultrasonic backscattering in polycrystals. *Ultrasonics* **54**.7 (2014), 1789–1803.
[48] L. Yang, J. Li, and S. I. Rokhlin. Ultrasonic scattering in polycrystals with orientation clusters of orthorhombic crystallites. *Wave Motion* **50**.8 (2013), 1283–1302.
[49] C. M. Kube and J. A. Turner. Acoustic attenuation coefficients for polycrystalline materials containing crystallites of any symmetry class. *The Journal of the Acoustical Society of America* **137**.6 (2015), 476–482.
[50] S. I. Rokhlin, J. Li, and G. Sha. Far-field scattering model for wave propagation in random media. *The Journal of the Acoustical Society of America* **137**.5 (2015), 2655–2669.
[51] A. Boström, P. Olsson, and S. K. Datta. Effective plane wave propagation through a medium with spheroidal inclusions surrounded by thin interface layers. *Mechanics of Materials* **14**.1 (1992), 59–66.
[52] S. K. Kanaun and V. Levin. *Self-consistent methods for composites: Vol. 2: Wave propagation in heterogeneous materials*. Springer, Dordrecht, 2009.
[53] A. Boström. Multiple scattering of elastic waves by bounded obstacles. *The Journal of the Acoustical Society of America* **67**.2 (1980), 399–413.
[54] A. Jafarzadeh, P. D. Folkow, and A. Boström. “Scattering of elastic SH waves by transversely isotropic sphere”. *Proceedings of the International Conference on Structural Dynamic , EURODYN*. Vol. 2. 2020, pp. 2782–2797.
[55] A. Jafarzadeh, P. D. Folkow, and A. Boström. Scattering of elastic waves by a transversely isotropic sphere and ultrasonic attenuation in hexagonal polycrystalline materials. *Wave Motion* **112** (2022), 102963.
[56] A. Jafarzadeh, P. D. Folkow, and A. Boström. Scattering of elastic waves by a sphere with cubic anisotropy with application to attenuation in polycrystalline materials. *Proceedings of the Royal Society A: Mathematical, Physical and Engineering Sciences* **479**.2272 (2023), 20220476.
[57] A. Jafarzadeh, P. D. Folkow, and A. Boström. Scattering of elastic waves by a sphere with orthorhombic anisotropy and application to polycrystalline material characterization. *Submitted for international publication* (2023).
[58] A. Jafarzadeh, P. D. Folkow, and A. Boström. Low frequency wave propagation in multiphase polycrystalline materials. *To be submitted for international publication* (2023).